Univerzita Karlova v Praze
Přírodovědecká fakulta

Studijní program: Biologie
Studijní obor: Buněčná a vývojová biologie – Fyziologie buňky

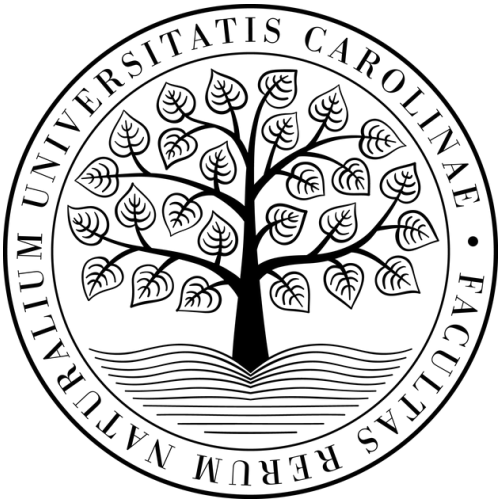

Bc. Markéta Sypecká

Editace leukemických B-buněk pomocí CRISPR/Cas9: hledání cílů miR-155 účastnících se procesu leukemogeneze

CRISPR/Cas9 editing of leukemic B-cells: searching for microRNA-155 targets involved in the process of leukemogenesis

Diplomová práce

Školitel: RNDR. Karina Savvulidi Vargová, Ph. D.

Praha, 2021

Prohlášení

Prohlašuji, že předkládanou diplomovou práci „Editace leukemických B-buněk pomocí CRISPR/Cas9: hledání cílů miR-155 účastnících se procesu leukemogeneze“ jsem vypracovala samostatně pod vedením RNDr. Kariny Savvulidi Vargové, Ph.D., s použitím odborné literatury a dalších informačních zdrojů, které jsou v práci citovány a uvedeny v seznamu použité literatury na konci práce.

V Praze dne 5.1.2021 Markéta Sypecká

Poděkování

Ráda bych poděkovala své školitelce RNDr. Karině Savvulidi Vargové, Ph.D. za trpělivost, věnovaný čas, odborné vedení a tematické připomínky k diplomové práci. Dále také děkuji Mgr. Eleně Golovině za veškerou její pomoc při zpracování mé diplomové práce a v neposlední řadě mým rodičům a přátelům, kteří mě během studia podporovali.

Contents

1. Introduction

1.1 Chronic Lymphocytic Leukemia (CLL)

Chronic Lymphocytic Leukemia (CLL) is an incurable disease, and one of the most frequent leukemias in developed countries. CLL is most frequently diagnosed among people aged 65–74, the median age at diagnosis is 70. (Chronic Lymphocytic Leukemia - Cancer Stat Facts, b.r.)

1.1.1 CLL Diagnosis, Prognosis, Treatment

Chronic Lymphocytic Leukemia is characterised by the accumulation of mature and CD5-positive B-cells – found in peripheral blood, bone marrow, spleen, and lymph nodes. CLL cells express following antigens CD19, CD20, and CD23 (Rozman & Montserrat, 1995). The most common revelation of Chronic Lymphocytic Leukemia is incidental discovery, mostly by routine examination. CLL is diagnosed by an elevated B-cell count in peripheral blood, estimated at more than 5000 B-cells per μL (Fig. 1). Which is 10-100 times higher than the usual concentration by a healthy person (Concentration of B cells in blood - Human Homo sapiens - BNID 103556, b.r.). The elevated count can be caused by other reasons e.g., infection. These reasons for lymphocytosis and lymphadenopathy have to be excluded, therefore immunophenotyping of peripheral blood is performed. In the case of immunophenotyping not being enough to diagnose, a biopsy of lymph nodes is executed.

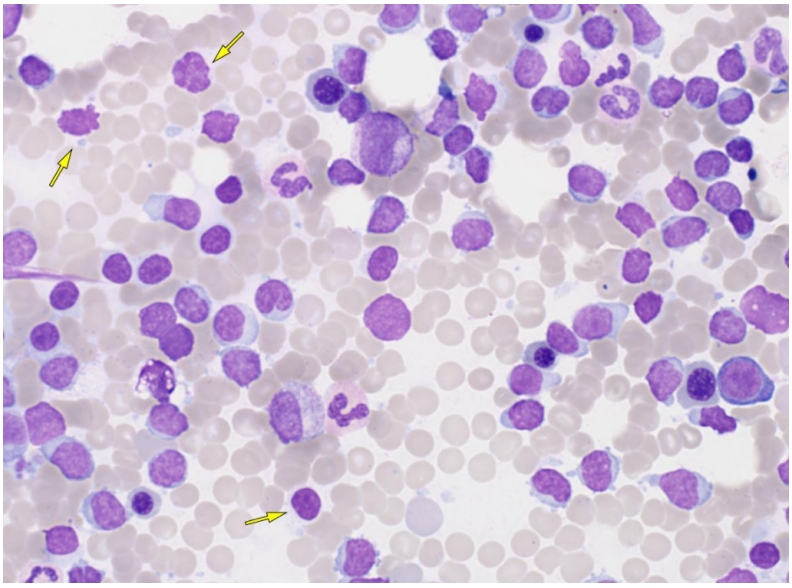

Fig. 1 Blood smear of bone marrow. Smudge cells, typical for chronical lymphocytic leukemia are shown in the picture by yellow arrows. (Picture was adapted from *Atlas of Haematological Cytology*, b.r.)

Prognosis

An international prognostic index for patients with chronic lymphocytic leukemia (CLL-IPI) („An International Prognostic Index for Patients with Chronic Lymphocytic Leukaemia (CLL-IPI)", 2016) was created to separate patients into four risk groups with a different chance of survival and planning of treatment – Low risk, Intermediate risk, High risk, and Very high risk. Separation into these four groups was performed based on specific genomic changes and chromosomal aberrations. Initial and most frequent aberration is the deletion of the 13q chromosome, which is present in 55 % of cases and trisomy of 12 chromosome. In more advanced stages, deletions of chromosome 11q and 17p occur (Rozman & Montserrat, 1995).

Genetic and molecular biology markers can be used for identification of the risk of progression and survival, which is complementary to the staging system. Mutations in specific genes vary according to the stage of the disease, for example, TP53 aberrations specifically occur by aggressive disease.

Besides the abovementioned genetic markers the CLL progression is also characterised by occurence of ZAP-70, CD38 molecules and on the mutation status of IgVH. Where the favorable CLL stage is described by ZAP-70-, CD38-, mutated IgVH and the adverse CLL stage is described by expression of ZAP-70, CD38 and unmutated status of IgVH (Chiorazzi et al., 2005)

Treatment

In the early stage of the disease, asymptomatic patients are monitored without therapy until disease progression. Basically, clinicians follow the rule "watch and wait"

Treatment of patients starts based on the Rai and Binet staging system and present symptoms, e.g., marrow failure, thrombocytopenia, unintentional weight loss.

Different types of chemoimmunotherapy drugs are used based on the patient’s fitness level and presence of *TP53* aberration. Treatment by a combination of drugs, such as anti-CD20 monoclonal antibody rituximab, fludarabine, and cyclophosphamide (FCR) helps the treatment and prolongs survival of patients. Patients with FCR treatment achieved the longest median progression-free survival, which leads to chemoimmunotherapy with FCR is the first-line standard care for physically fit patients (Cramer et al., 2016).

Patients with *TP53* aberration have a very aggressive disease course and respond poorly to chemoimmunotherapy. The outcome improved with the introduction of ibrutinib, idelalisib, and venetoclax, all of them act independently of the p53 pathway.

Choosing the right pathway for treatment may be difficult because of so many options. Therefore parameters that are considered include fitness, age, comorbidities, and genetic status of TP53 (Eichhorst et al., 2015).

Duration of remission varies however, 86,1 % of patients survive 5 years after the diagnosis of CLL (*Chronic Lymphocytic Leukemia - Cancer Stat Facts*, b.r.). Patients are regularly monitored and when symptoms occur, second-line treatment starts. The sooner relapse appears the poorer prognosis the patient has.

1.2 Characteristics of microRNAs

MicroRNAs (miRNAs) represent single stranded non-coding RNAs (ncRNAs) found in all kingdoms (plants, animals and viruses) and 18-25 nucleotides long (Mashima, 2015). MiRNAs are evolutionarily conserved among species that underlie their importance in biological processes (Bartel DP et al, 2018). The function of miRNAs lies in the regulation of gene expression by suppressing newly synthetised proteins through inhibition or destabilisation of mRNA (messengerRNA) in eukaryotes (Mashima, 2015).

1.2.1 Discovery

The first miRNA was discovered in 1993 by Ambros‘s and Ruvkun‘s groups in *Caenorhabditis elegans*, specifically lin-4, which is crucial in the larval development of *C. elegans* (Almeida et al., 2011). In 2000 was discovered second miRNA and there began outbreak of discoveries connected to miRNAs. Such as importance of DICER protein in miRNA pathway (Grishok et al., 2001; Hutvágner et al., 2001), connection between overexpression of miRNAs and cancer. Using anti-miR for therapy. Overexpression of a single miR is sufficient to cause cancer (O’Donnell et al., 2005).

Silencing of the target gene is based on Watson-Crick base pairing of the miRNA with 3’UTR of the gene.

1.2.2 Biogenesis of miRNAs

Most mammalian miRNAs are transcribed in the genome at first in the form of long primary transcripts (pri-miRNAs) by RNA polymerase II. The pri-miRNAs consist of cap structure at the 5' end, one or more hairpin structures and polyadenylated 3' end. Pri-miRNAs can be spliced in more ways, which leads to generating more than one functional miRNA (Carthew and Sontheimer, 2009). In the nucleus, the pri-miRNAs are processed by RNAse II endonuclease III Drosha enzyme and DGCR8/Pasha protein, a double-stranded RNA-binding domain protein. After the excision precursor-miRNA (pre-miRNA) is formed and exported from the nucleus by Exportin 5 protein. After the displacement of pre-miRNA into the cytoplasm, pre-miRNA is cleaved by Dicer protein (Carthew & Sontheimer, 2009). The pre-miRNA in duplex form binds to a protein of the Argonaute (Ago) family to build an RNA Induced Silencing Complex (RISC). Regulation of miRNA biogenesis has not been extensively studied yet. The process of miRNA biogenesis described above shows Fig. 2.

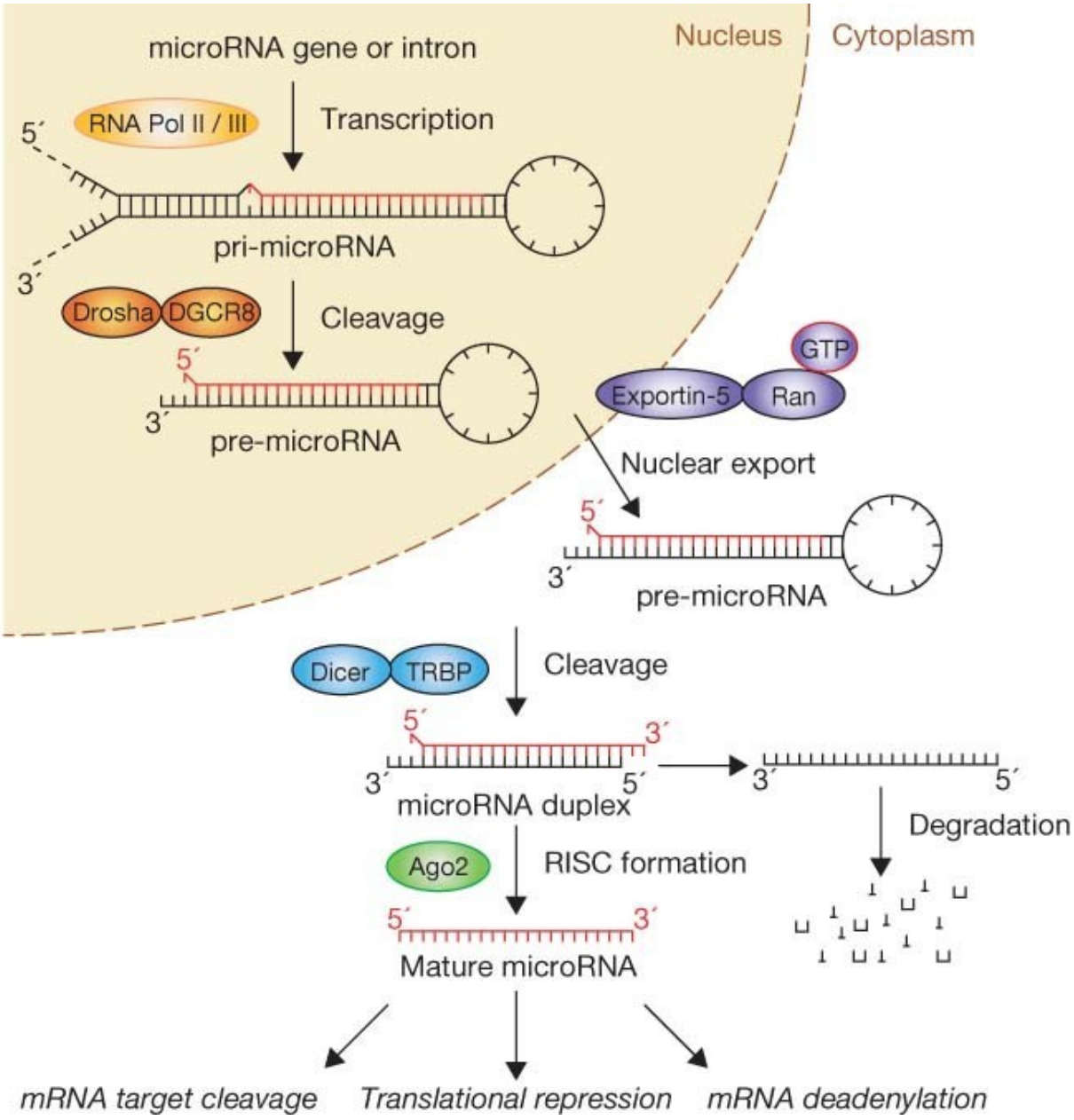

Fig. 2 Biogenesis of miRNA. Canonical processing pathway of miRNAs starts in nucleus, firstly there is primary miRNA (pri-miRNA), after cleavage by Drosha-DGCR8 complex pre-miRNA is formed and later exported to cytoplasm and cleaved further until the mature miRNA is formed. (Figure adapted from (Winter et al., 2009)

1.2.3 Mechanism of function

Further is described the mechanism of miRNA function only in animals, not plants (there is a different mechanism of miRNAs action). Binding of miRNA in RISC (miRISC) is important for specific recognition of target mRNA. Generally, miRNA-binding sites are set in 3'UTR (untranslated region) of mRNA in multiple copies. MiRNA is bound to these sites by Watson-Crick base pairing in length of 2-8 nucleotides – which is called as seed region.

According to the level of miRNA-mRNA complementarity the way of suppressing the gene is chosen – perfect complementarity allows cleavage of the mRNA strand. If central mismatches occur, cleavage does not happen, but the translation of mRNA is repressed. Guo et al. found out, that inhibition of translation had just slight effect compared to destabilization of mRNA (H. Guo et al., 2010). It is unclear if the repression occurs in initiation of translation or in the later phase. There are three models of possible repression by miRISC, the first is competition of miRISC and eIF4E for binding to 5' cap structure. The second is deadenylation, therefore destabilizing the mRNA, and the third is miRISC blocks the association of large and small ribosomal subunits (Chendrimada et al., 2007). MiRNAs can also act as transcription activators by binding to enhancer sequences (Xiao et al., 2016).

1.2.4 MiR-155 expression in hematopoetic cells

The sequence coding mature miR-155 is highly conserved in humans, mice and chickens (Mashima, 2015), MiR-155 physiologically involves in the lymphoid and myeloid cells development where the levels of miR-155 differ depending on the cell type (Georgantas et al., 2007). During the erythroid differentiation *in vitro*, there was proven, that the level of miR-155 was 200 fold lower in mature red cells, and miR-451 was upregulated at the same time. Demonstrating, that these two miRNAs are crucial for differentiation in myelopoiesis and erythropoiesis (Georgantas et al., 2007).

One of the roles of miR-155 is maturation of B-cell and T-cell. MiR-155 is known as oncomir to many types of leukemias/cancers, such as Hodgkin Lymphoma and subtypes of Non-Hodgin lymphomas (Eis et al., 2005; Kluiver et al., 2005). MiR-155 is also involved in inflammatory pathways. The B-cell development is directly affected by transcriptional factors, which are connected to miRNAs. Deregulated expression of miRNAs and transcription factors are key events in pathogenesis of B-cell malignancies(Fabbri & Croce, 2011). In physiological lymphopoiesis, the highest level of miR-155 is expressed in germinal center cells, intermidiate level hematopoietic stem cells and the lowest mature B-cells (Georgantas et al., 2007). It has been reported that direct target of miR-155 is *SHIP1* (Src homology-2 domain-containing inositol 5-phosphatase 1) gene that regulates differentiation of B, T-cells and macrophages (O'Connell et al., 2011).

Mouse models of miR-155

Until now it was generated four main miR-155 transgenic mouse models with either enhanced (Costinean et al., 2006) or deficient miR-155 expression (Thai et al., 2007; Vigorito et al., 2007). More information about mechanism of miR-155 acting in immune system may help to understand its role in leukemic process.

In the miR-155 over-expressing transgenic mice ("Eμ–mmu-miR-155" mouse model), pre-leukemic stage with polyclonal B-cell expansion and splenomegaly developed initially (after 3 weeks). Later, after seven month, pre-leukemic stage progressed into high-grade B-cell lymphoma that is direct evidence of miR-155 functioning as activator of leukemia development(Costinean et al., 2006)

Vigorito *et al.,* confirmed importance of miR-155 in antibody production in germinal centers (Vigorito et al., 2007). MiR-155 deficient mice had reduced proportion (50%) of germinal center B-cells that led to reduced production of high affinity antibodies. Interestingly, authors firstly thought that impaired antibody production is result of dysfunctioning of somatic hypermutation affected by miR-155. The further experiments showed that miR-155 does not affect somatic hypermutation that occurs in germinal center B-cells (Vigorito et al., 2007). Failure of antibody production is due to block in differentiation of plasmablast B-cells (stage of B-cells between plasma and mature B-cells) and in reduced production of cytokines. This was confirmed also by other groups of researchers as Thai and Rodriguez(Rodriguez et al., 2007; Thai et al., 2007). Moreover, the miR-155 deficient mice produced less amount of IgM and switched antigen specific antibodies after immunization with pathogen – *Salmonella typhinurium*. The evidence that miR-155 regulates also T-cells represents its strong up regulation in activated T-cells (Thai et al., 2007). Rodriguez *et al.,* also proved that dendritic cells failed efficiently activate T-cells (Rodriguez et al., 2007).

As the miR-155 bears the potential to be therapy-targeted molecule, Babar *et al.*, generated miR-155 Cre-loxP tetracycline controlled knock-in mouse model (miR-155^{LSLtTA}). In these mice, the transcription of miR-155 can be deactivated by doxycycline, thus it provides "TET OFF" system with temporal controlling of miR-155 transcription. MiR-155 ^{LSLtTA} mice developed after five month disseminated lymphoma with enlarged lymph nodes and splenomegaly. Surprisingly, mice with such miR-155 induced lymphoma after

doxycycline treated food displayed within two days reduced lymph nodes and in 2 weeks the lymphoid organs were as in normal, healthy mice (Babar et al., 2012).

To summarize, over expression of miR-155 leads to high grade B -cell lymphoma and miR-155 knockout mice model showed on a marked impairment of miR-155 in T- and B-cell function. The knock-in mouse model gave strong evidence that miR-155 is inductor of B-cell leukemia. Moreover, miR-155 regulates homeostasis of immune system, thus it makes potentially very powerful therapy tool.

Regulatory role of miR-155 and its targets

The number of target genes according to miRTarBase is 3287 (January, 2021), which supports the fact that miR-155 represents multifunctional miRNA. Some of miR-155 target genes are shown in figure 3, showing, that miR-155 is not extended just by number of target genes, but also by the location of function of target genes.

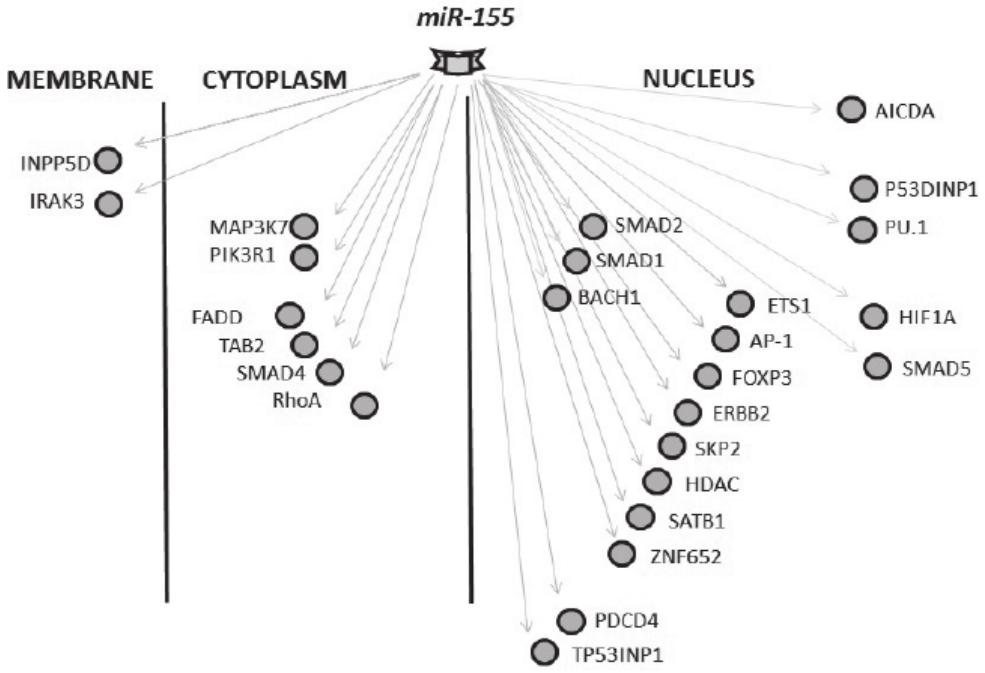

Fig. 3 Schematic view of miR-155 targets. Target genes modulated by miR-155 in malignant development and progression are included in group of transcription factors located in nucleus (e.g. PU.1), kinases in cytoplasm (e.g. MAP3K7), binding proteins (e.g. SATB1), membrane bound proteases (e.g. INPP5D), and proteases, kinases and enzymes in cytoplasm. (Adapted from (Jurkovicova et al., 2014)

The group of Yu et al.found out, that just in colorectal carcinome, the miR-155 is responsible for regulating the proliferation, cell cycle, apoptosis and migration of colon cancer cells (Yu et al., 2017). The inhibition of apoptosis by affecting by PTEN pathway was confirmed in psoriasis by (Xu et al., 2017). Knockout of miR-155 in mice lead to attenuation of immune system (Vigorito et al., 2013).

Out of these miR-155 targets, only a few are related to B cell development, cell cycle, differentiation, and CLL pathogenesis. Certain targets (such as *PU.1* and proto-oncogene *MYB* transcription factors) belong to the group of so-called "master regulators" of gene expression in hematopoiesis. *PU.1* controls the process of hematopoietic cells differentiation in a dose-dependent manner (DeKoter & Singh, 2000). In a case of B cell differentiation, a low level of PU.1 restrains B cell production. At a higher level, PU.1 blocks the differentiation of B cells into plasma cells (Lu et al., 2014; Vigorito et al., 2013). Previously group of Vargova et al. described the direct negative relationship between the elevated level of miR-155 and downregulation of PU.1 in CLL(Huskova et al., 2015; Pospisil et al., 2011; Vargova et al., 2017) (Vargova et al. 2011, Huskova et al. 2015, Vargova et al, 2017). A recent study shows that miR-155 affects mitosis and chromosomal stability during tumorigenesis. The authors described novel targets of miR-155 that interact with cell cycle regulatory proteins. The mechanism of miRNA action on genome stability and ploidy is still described scarcely.

The question of how miRNAs orchestrate the cell fate through their respective targets in CLL remains enigmatic. Answering this question is crucial for the understanding of the molecular network of CLL leukemogenesis.

Genome editing technology using clustered regularly interspaced short palindromic repeats (CRISPR/Cas9) becomes today's routine method for fast and precise editing of any gene of interest. Successful usage of this novel technology in large-scale in practically all research fields was described .Until now, there are only a few research papers describing the usage of this technology for the editing of miR-155 (Pagotto et al., 2018; Wallace et al., 2017).

1.3 Gene editing technology – CRISPR

Abbreviation **CRISPR** means **C**lustered **R**egularly **I**nterspaced **S**hort **P**alindromic **R**epeats. Presence of these repeats is used as a defense mechanism against viruses in bacteria and archaea. Originally CRISPR was described by Yoshizumi Ishino in 1987, who discovered it accidentally. At that time the function of CRISPR was unknown.

In 2000 Mojica identified interrupted direct repeats in other species of bacteria and proposed the acronym CRISPR that is used until now.

With abovementioned palindromic repeats in CRISPR system are tightly associated proteins, which are called Cas – **C**RISPR **As**sociated Protein (Cas). There are two classes I and II that subdivides into types. Formerly only four types were known. Recently there are described six types (Makarova & Koonin, 2015; Mohanraju et al., 2016). The most known and applied in research is Cas9 type which is also used in this thesis. Cas proteins have helicase and nuclease activity which is used during the excision of targeted DNA.

1.3.1 Introduction to CRISPR technology - history

In 2005 three independent research groups figured out that CRISPR spacers have the origin in viral DNA, based on the presence of sequences root from previous infections (Grissa et al., 2007; Horvath & Barrangou, 2010; Marraffini & Sontheimer, 2010). This prompted them to the idea that CRISPR could be a part of adaptive immunity in bacteria.

In 2007 was experimentally proven that CRISPR is a part of the adaptive immunity system, when they transferred resistance to a different clone of *Streptococcus thermophilus* by deleting and adding spacers (R. Barrangou et al., 2007; Hille et al., 2018; Lander, 2016; Morange, 2015).

Emmanuelle Charpentier and Jennifer Doudna received in 2020 Nobel Prize in Chemistry for adapting CRISPR/Cas9 system and using it for genome editing. They changed the four-component Cas9 endonuclease into two-component, which is easier to handle. This artificial system has the ability programmed bind to any target DNA sequence and cut at a specific place (Garneau et al., 2010). Also group of Virignijus Šikšnys reprogrammed the target site, so it was possible to bind target DNA, by changing the sequence of crRNA- crispr RNA.

In 2013 CRISPR was successfully used on mammalian cells. First one who described genome editing by CRISPR/Cas9 was group of Feng Zhang and George Church, who edited human cell culture (R. Barrangou et al., 2007; Rodolphe Barrangou, 2015; Deltcheva et al., 2011) . CRISPR editing technique was then widely spreaded in another species of mammals, such as mice, monkeys and human embryos (X. Guo & Li, 2015; H. Wang et al., 2013).

3.2 Mechanism of CRISPR function in *Mammalia*

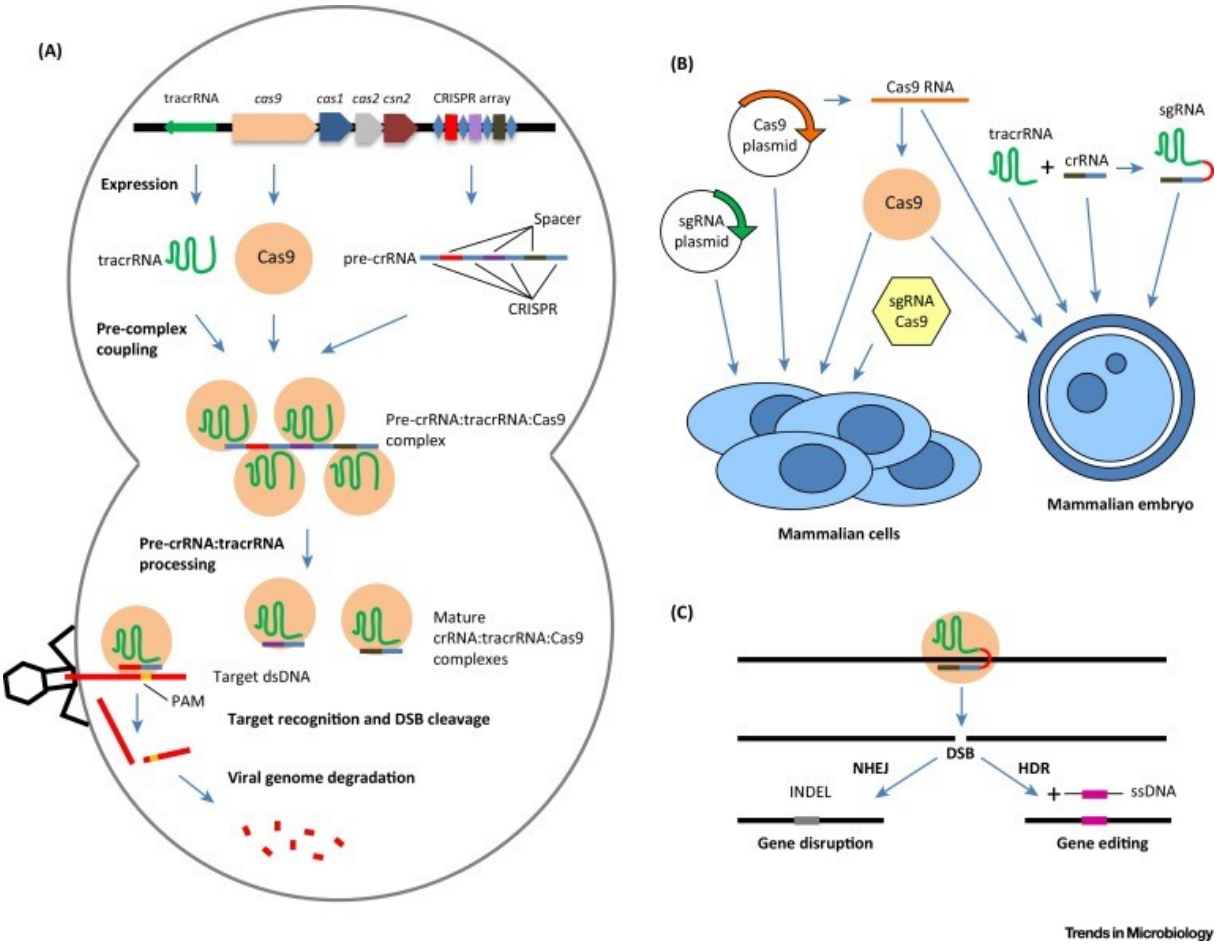

Fig. 4 CRISPR/Cas9 system of function (Mojica & Montoliu, 2016) Not drawn to scale. *In* (A) is presented the naturally occurring Type II CRISPR-Cas system in Streptococcus pyogenes and the mechanism of defense against viruses. (B) The crucial parts were taken and assembled in a few or one plasmid cassette. These are then used in mammalian cells or embryos. (C) CRISPR-Cas9 system develops double-strand break in the target DNA. In order to repair this break, cells perform two endogenous mechanisms of fixing, NHEJ – Non-Homologous End Joining, which is connected to deletion or insertion of nucleotides, leading to gene disruption. The second option is HDR- homology-directed repair, which requires a matrix in order to be copied (Mojica & Montoliu, 2016). There are different ways how to insert these particles or plasmids into cells, such as transduction via lentivirus or adeno-associated virus, also microinjection or electroporation.

1.3.2 Editing of miRNAs by CRISPR

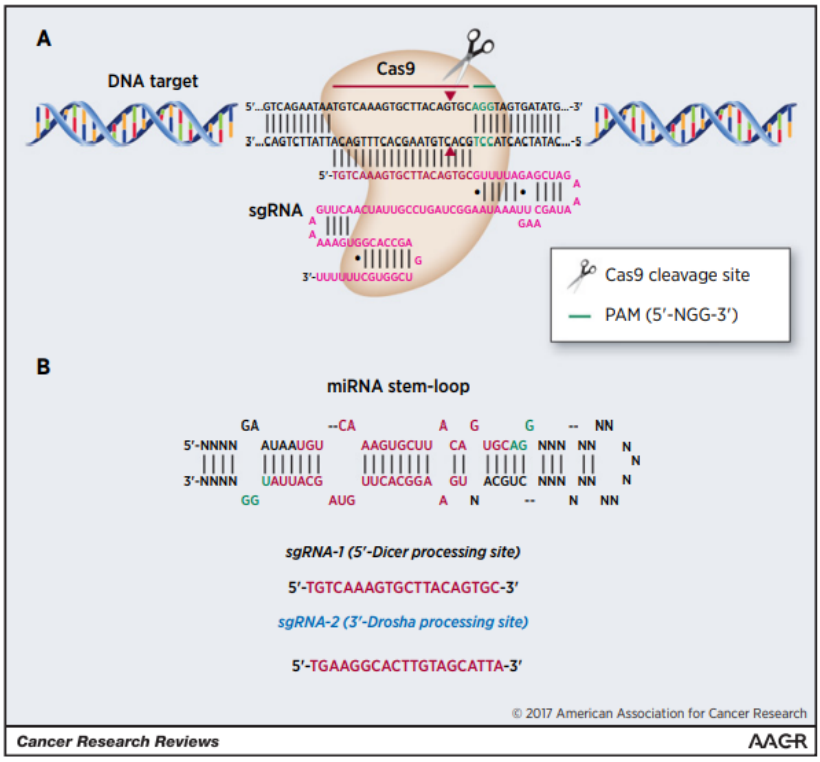

Figure 1.
Schematic diagram of the mechanism of CRISPR/Cas9-mediated miRNA editing. **A,** The Cas9 nuclease from *S. pyogenes* is targeted to genomic DNA (e.g., the *hsa-miR-17* gene) by an sgRNA consisting of a 20-nt guide sequence (red) and a scaffold (magenta). The guide sequence pairs with the DNA target (red line on top strand) directly upstream of a required 5′-NGG adjacent motif (PAM; green). The Cas9 nuclease introduces a DSB in targeted genomic DNA (e.g., Drosha or Dicer processing sites) approximately 3 bp upstream of the PAM (red triangles). The DSB generated by Cas9 is repaired by host-mediated DNA repair mechanisms. nt, nucleotide; bp, base pairs. **B,** CRISPR/Cas9 can alter the biogenesis process of miRNA. SgRNAs targeting the sequences within/adjacent to Drosha- and Dicer-processing sites, respectively, in the secondary stem-loop structure of primary miRNA sequences can lead to the reduction of mature miRNAs in cells. Both arms of the mature miR-17 sequence in the stem-loop of the hairpin are depicted in red. PAM sequences are highlighted in green. The mechanism of editing of *hsa-miR-17* mediated by sgRNA-1 is depicted in **A**.

Fig. 5 (*Emerging Role of CRISPR/Cas9 Technology for MicroRNAs Editing in Cancer Research | Cancer Research*, b.r.)

Using CRISPR/Cas system in gene editing is highly appreciated because of its easy design, high targeting efficiency and almost none off-target mutations. CRISPR/Cas9 system is versatile and used among many species for its high-throughput and multiplexed gene-editing approaches (Friedland et al., 2013; Kistler et al., 2015). Cas9 protein binds to DNA by specific pairing of sgRNA bound to the target DNA sequence. CRISPR/Cas9 system performs double strand break of the target DNA three base pairs upstrem to PAM sequence (shown in Fig. 5). During gene-editing, there is used the selfability of the cell to repair the double DNA break by its endogenous repair machinery, this gene-editing technique is used also in *in vivo* and *in vitro,* in order to investigate more human diseases (Chang et al., 2016; SHAO et al., 2016).

As was mentioned before in part 2.4.2 „Regulatory role of miR-155 and its targets“ in miRNA expression could lead into cancer. Gene editing by CRISPR is also used for curing different types of cancer by modulating the miRNA expression. Successful gene editing of specific miRNA sequences resulted in changes of its targets - mainly oncogenes, was performed on cells from renal cell carcinoma, pancreatic cancer and chronic myeloid leukemia (He et al., 2014; Y. Wang et al., 2012; Yoshino et al., 2017).

Using CRISPR as therapeutic tool concerns non-target loss of function by deleting miRNAs, which are cancer/leukemia specific. To avoid this concerns, there is possibility to use tissue-specific promoters. Another possibility is to use modified Cas9 - edited in its nuclease activity to perform only nicks in one strand instead of double strande break. Decreasing the size of sgRNA lowers off-target binding (Fu et al., 2014).

On the other hand, targeting only miRNA sequences may not be sufficient for therapeutic purposes. Because in some diseases, specially cancer, there is malfunction of pathways including few genes, not just one. Previously, Kabadi and colleagues (Kabadi et al., 2014) used a Cas9 in plasmid with four different sgRNAs and successfully sustained transcriptional activation. The way of delivering the plasmid may still cause some difficulties especially in primary cells or leukemic B cells and deserving more attention.

2. Hypothesis

Imbalance in miRNA expression represents one among many factors that initiate leukemia/cancer. OncomiR-155 is highly expressed in many leukemias/cancers, including CLL. The process of leukemogenesis is associated with changes in the gene expression profile of mRNAs, the miRNAs targets. Elevated levels of miR-155 results in suppression of its targets.

We hypothesize that by gene editing of CLL B - cells we unblock miR-155 targets and find out correlation between these targets (known and also unknown) in CLL during leukemia progression.

2.1 Aims of the thesis

1. By CRISPR/Cas9 tool create deletion mutant of human B-CLL cell line HG-3 that does not express miR-155.

2. Explore the impact of miR-155 deletion on HG-3 cell line viability and proliferation.

3. Perform qRT-PCR to compare the gene expression profile of HG-3 cells before and after gene editing.

2.2 Specific aims of the thesis

1. What kind of differences we can detect in the transcriptom of CLL cell line HG-3 and MEC-1 after deletion of miR-155 by CRISPR/Cas9 in these cells? (up/down expression of miR-155 targets; validated/novel)

2. Show HG-3 and MEC-1 similar trend in the proliferation rate before and after miR-155 editing by CRISPR/Cas9?

3. Material and Methods

In all experiments performed in this thesis, the HG-3 and MEC-1 cell lines were used. HG-3 cell line is derived from a Caucasian man diagnosed with an early stage of Chronic Lymphocytic Leukemia disease. MEC-1Experiments with MEC-1 cell line were performed earlier by Dr. Savvulidi Vargová. Both cell lines were treated with nucleofection and insertion of plasmid, which consisted of Cas9 (CRISPR associated protein 9), gRNA (guide), GFP (green fluorescence protein) for identification and resistance against antibiotics (Kanamycin).

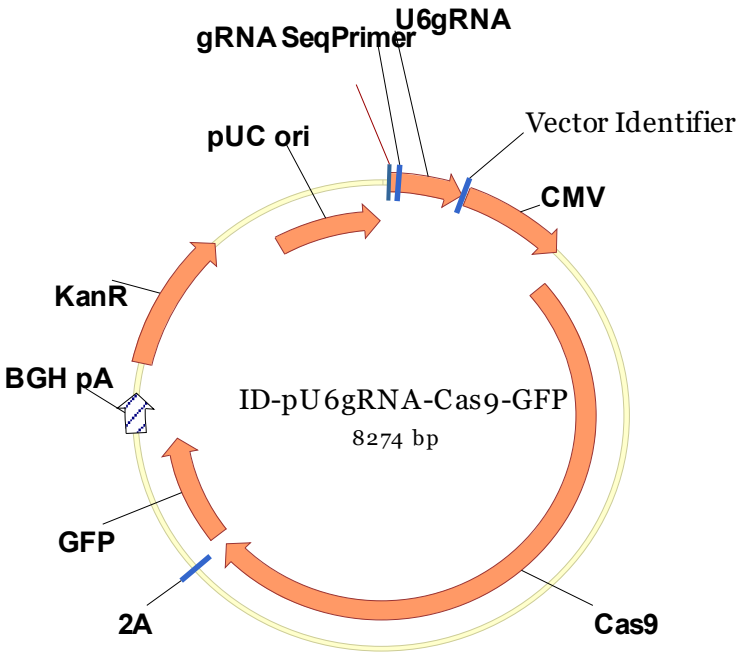

Fig. 6 Plasmid used for CRISPR/Cas9 gene editing - U6gRNA-Cas9-2A-GFP MiR155.

Afterwards the viable cells that contained GFP were selected by Fluorescence-activated cell sorting. Clones of GFP positive HG-3 cells were cultivated for 3-4 weeks after nucleofection. After that, cryopreservation, DNA and RNA isolation were performed.

Isolated DNA was multiplied by Polymerase Chain Reaction (PCR), then transferred to 2% Agarose electrophoresis gel. The PCR product of the desired length was isolated from the gel and sequenced (Sanger sequencing) to verify if desired deletion of 22 nt responsible for mature miR-155 was successful.

Isolated RNA of gained clones with deletion of sequence for mature miR-155 was used for Quantitative Reverse Transcription Polymerase Chain Reaction (qRT-PCR). This PCR product – complementary DNA (cDNA) was utilized for measuring the changes in transcriptome. The transcriptome of clones was measured and verified by qPCR.

3.1 Material

3.1.1 Biological material

HG-3 Cell line

HG-3 cell line is derived from a 70year old Caucasian man diagnosed with an early stage of Chronic Lymphocytic Leukemia disease (Rai stage II). HG-3 cell line was obtained from DSMZ (Deutsche Sammlung von Mikroorganismen und Zellkulturen – German Collection of Microorganisms and Cell Cultures). Morphology of HG-3 cells is described as round suspension cells partly growing in clumps and slightly adherent. Its doubling time is between 50 and 60 hours. The imunology profile is negative in these clusters of differentiation: CD3, CD4, CD10, CD13, CD34; positive in these: CD5, CD15, CD19, CD20, CD37, CD80; HLA−, DR+, cyIgG−, cyIgM+, cyκ−, cyλ+.

The karyotype is near-diploid: 46(44-46)<2n>XY, der(10)t(10;11)(q26;q24.1), del(13)(q12q32), there is marginal resemblance to original karyotype. The karyotype consists of 44-46 chromosomes including XY chromosomes, derivative chromosome 10 consisting of q26 part of 10^{th} chromosome and q24.1 part of 11^{th} chromosome; deletion of the13^{th} chromosome is present between q12 and q32 part of the chromosome.

MEC-1 cell line

MEC-1 cell line was established in 1993 from the peripheral blood of a 61-year-old Caucasian man with chronic B cell leukemia (B-CLL in prolymphocytoid transformation to B-PLL. HG-3 cell line was obtained from DSMZ (Deutsche Sammlung von Mikroorganismen und Zellkulturen – German Collection of Microorganisms and Cell Cultures). Morphology of MEC- 1 cells is described as round to polymorphic cells growing in suspension, singly or partly in small aggregates, a few cells are slightly adherent. . Its doubling time is around 40 hours. The imunology profile is as follows: CD3 -, CD10 -, CD13 -, CD19 +, CD20 +, CD34 -, CD37 +, CD38 +, cyCD79a +, CD80 +, CD138 +, HLA-DR +.

The karyotype is near-diploid with 10% polyploidy - 46(44-47)<2n>XY, -2, +7, -12, +1-2mar, t(1;6)(q22-23;p21), add(7)(q11), der(10)(10pter->q22::?::2q11->qter), del(17)(p11) - small acf/mar present in most cells - resembles published karyotype.

3.1.2 Chemicals and buffers

Dimethylsulfoxid(DMSO)	Sigma-Aldrich
Fetal Bovine Serum (FBS)	Biosera
Isopropylalkohol p.a.	Sigma-Aldrich
Penicilin-Streptomycin (100x)	Sigma-Aldrich
Phosphate Buffered Saline (PBS) (10x)	Biosera
Propidium iodid (PI)	Sigma-Aldrich
RPMI 1640 medium	Biosera
TRI reagent	iBioTech
plasmid U6gRNA-Cas9-2A-GFP MiR155	Sigma-Aldrich
GeneRuler 100 bp Plus DNA Ladder	Thermo Scientific

Commercial kits

Amaxa™ Human B Cell Nucleofector™ Kit	Lonza
DNeasy Blood & Tissue kit	Qiagen
QIAEX II® Gel Extraction Kit	Qiagen
TaqMan Universal PCR Master Mix	Thermo Fisher Scientific

Plasmids

Plasmid which was used for CRISPR/Cas9 reaction is U6gRNA-Cas9-2A-GFP MiR155. The original amount was inserted in *E.coli* and isolated in higher amount later.

3.1.3 Instruments

Amaxa nucleofector Device II	Lonza
BD FACS Aria IIu cell sorter	BD Biosciences
BD FACS Canto II fluorescence analyser	BD Biosciences
Bioanalyzer 2100	Agilent Technologies
iBlot Gel Transfer System	Life Technologies
Mastercycler Gradient	Eppendorf
7900HT Fast Real-time PCR System	Life Technologies
ChemiDoc™ Imaging System	

3.2 Methods

3.2.1 Cultivation of HG-3 cell line

HG-3 cell line was cultivated in medium made out of RPMI, 10 % of FBS and 1 % of antibiotics – penicilin/streptomycin. The temperature was 37°C and concentration of CO_2 5%. Concentration of the cells was between 0,5-1 million cells per mililiter. Culture medium was changed every 2 - 3 days.

Transfection of HG-3 Cells by Amaxa nucleofector

Procedure/method

One day prior nucleofection

1. Firstly the cell number was determined. For one nucleofection reaction $2x10^6$ cells was used.
2. Cells were cultured in RPMI medium supplemented with 10 % of FBS, without P/S, 24 hours prior nucleofection. For each well 2 ml of this complete medium was used.
3. Cells were cultured in humidified incubator with 5 % CO_2 and 37°C.

Day of nucleofection

1. Plasmids which were used:
    a. GFP (pMAX GFP, Amaxa nucleofection kit) c = 0,5 µg/µl as positive control; 2 µg per reaction
    b. CRISPR/Cas9/miR-155 c = 1 µg per reaction
    c. CRISPR/Cas9/miR-155 c = 2 µg per reaction
2. Nucleofection solution was prepared. For each reaction 100 µl of complete nucleofection solution was used. Complete nucleofection solution was mixed in ratio of solution:supplement 4,5:1. Nucleofection solution was kept in room temperature in laminar hood.
3. Prepared RPMI medium (without P/S) was preheated at 37°C and divided in 6 well plate; 2 ml of medium per well.
4. Cells were spinned down in eppendorf tubes for 5 minutes, in room temperature with velocity 1900 rpm (300 rcf). Supernatant was discarded and the cell pellets were kept on ice.
5. For nucleofection of HG-3 cells by Amaxa nucleofector, nucleofection kit #VPA-1001 and program U-015 were used.

3.2.2 FACS – Fluorescence Activated Cell Sorting and Gaining of the Clones

24 hours after nucleofection desired cells were sorted out by flow cytometry (FACS ARIA II, BD FACSDiva 8.0.1). By sterile single-cell sorting only GFP positive (wavelength 510 nm) and propidium iodid negative (wavelenght 617 nm) cells were sorted out in 96 well plate (Fig. 7).

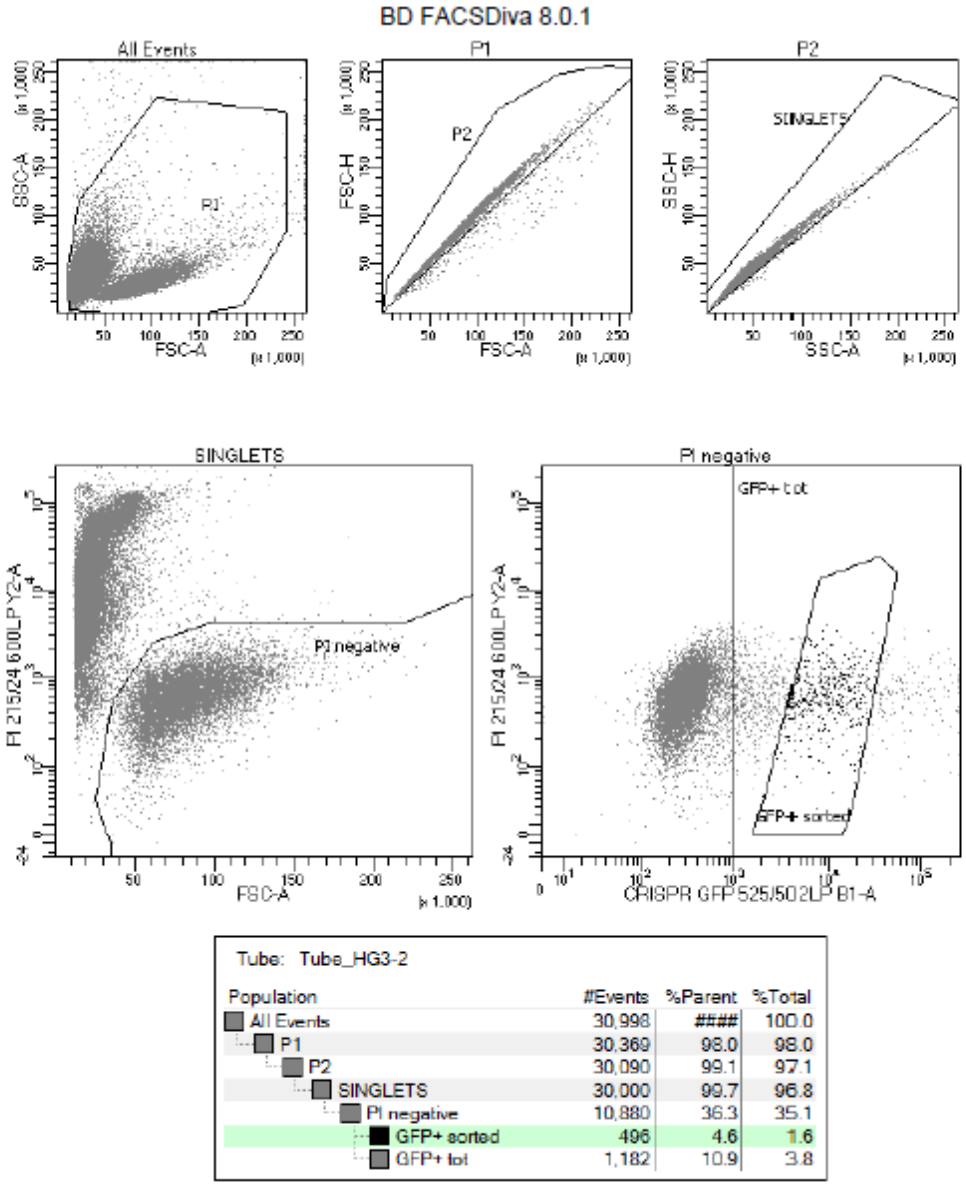

Fig. 7 Presentation of perfomed FACS sorting.

Sorted single-cells were cultivated in RPMI medium supplemented with 10 % FBS and 1% P/S in humidified incubator with 5 % CO_2. The single cell clones were harvested (after 3-4 weeks of culturing) when the cells reached density around 500 000 cells per mililiter to perform DNA and RNA isolation.

3.2.3 Sequencing

Sanger sequencing was performed in BIOCEV facility.

DNA Isolation

DNeasy Blood & Tissue Qiagen kit for DNA isolation was used and followed the manufacturer`s protocol: Purification of Total DNA from Animal Blood or Cells (Spin-Column Protocol) with some modifications.

Protocol for cultured cells was followed and the amount of $5x10^6$ cells was used. Firstly the cells were cleaned by centrifugation at speed 14 000 rpm (20 817 G) in PBS for 5 minutes at room temperature. The supernatant was discarded. Then the instructions were followed. Ethanol (96 %) was used. At step 7 in protocol 100 µl of nuclease-free water (preheated at 56°C) instead of Buffer AE was added into the spin column. This eppendorf tube with spin column was left for 5 minutes at room temperature, spinned down for 1 minute at 8 000 rpm (6797 G), at room temperature. Concentration of DNA was measured by Nanodrop spectrophotometer. The gained DNA was stored at 4°C for short term and at -20°C for long term.

PCR reaction – preparation of product for Sanger Sequencing

Isolated DNA from the previous step was multiplied by Polymerase chain reaction. Because this PCR product was later needed for sequencing, AccuTaq™ LA DNA Polymerase was used. The protocol below for the PCR was pursued. The quantity of gDNA was 100 ng, which differed in the volume of µl, according to the concentration of DNA in the isolated solution. Altogether the amount for H_2O and DNA solution was 11.8 µl. For gaining aspecific sequence of mature miR-155 with the length of 358 bp, unique primers were designed (Vector NTI software).

The sequences of primers were following:

Primers	Sequence	Tm
Forward primer	CTCCAGCTTTATAACCGCATCTGC	58°C
Reverse primer	GTTGAACATCCCAGTGACCA	50°C

Whole reaction mixture consisted of following components:

Reaction:	1x

Program of the reaction was following:

Program:			
	98°C	30 sec	
	94°C	10 sec	
	60°C	20 sec	35 cycles
	68°C	1 min	

Accutaq LA 10x buffer	2.0
dNTPs (2.5 mM each, final 10mM)	4.0
DMSO (final c=2%)	0.4
primer F+R 10uM PCR/Seq	1.6
Accutaq LA 10x polymerase	0.2
H_2O (nuclease-free)	10.8
gDNA (100 ng/µl)	1.0
Total	20.0

	60°C	10 min
	4°C	1 min
	4°C	hold

Gel electrophoresis

For gel electrophoresis 2 % agarose gel was used. Gel was prepared with TBE solution and 2.5 µl of ethidium bromide was added per 50 ml of gel. Loading dye was diluted 6 times in PCR product and this mixture was loaded on agarose gel (20 µL/lane). Electrophoresis lasted one and half hour, with 80 V. For detection of PCR product size DNA ladder 100 bp was used.

Detection of PCR product

Runned agarose gel was viewed by ChemiDoc™ Imaging System to check the size of PCR product. Desired band with proper size of PCR product was cutted out from gel under UV light. Afterward DNA was isolated by gel extracation kit.

DNA extraction from gel

For DNA extraction of desired length from gel commercial QIAEX II® Gel Extraction kit was used. The manufacturer`s protocol only with small modification was carefully followed. Modification was done in 9th step where instead of TE buffer the preheated at 56°C nuclease-free water was used.

Gene expression

RNA Isolation

Before starting the RNA Isolation all of the surface and pipettes were cleaned by Nuclease Eliminator solution.

1) Cells were harvested, until the amount of $5x10^6$ cells was reached. This amount was centrifuged for 5 minutes at room temperature.

2) Pellet was resuspended in TRI reagent and left for 5 minutes to complete cell lysis, on bench at room temperature.

3) To the TRI reagent cell suspension 100 µl of chloroform ($CHCl_3$) was added. This was mixed by vortexing for 2 seconds and left for another 5 min on the bench. After this, the mixture was centrifuged at 11000 rpm (13552 rcf) for 15 min at 10°C.

4) The clear upper phase (~250 µl) was transfered into a new eppendorf tube and mixed with the same amount of $CHCl_3$, vortexed and centrifuged at 11000 rpm for 7 min at 10°C.

5) The clear upper phase was transfered into new eppendorf tube and 1 µl of linear acrylamid, 250 µl of Isopropanol was added. This was vortexed, shortly spinned and precipitated at −20 °C overnight.

6) The other day the tube was shortly vortexed and centrifuged at 14000 rpm for 30 min at 4 °C.

7) The supernatant was decanted, to the pelet 500 µl of 75 % ethanol was added, vortexed gently and centrifuged at 14000 rpm for 5 min at 4 °C.

8) Supernatant was again decanted, mixture was spinned down shortly and removed rest of the liquid completely, left the pellet to dry on the air for 3-5 min covered with a paper towel.

9) The RNA pellet was in 12 µl of nuclease free water with RNAse inhibitors (1 %) dissolved and analyzed by Nanodrop.

The RNA was stored at −80°C.

cDNA synthesis (RT-PCR – reverse transcriptase polymerase chain reaction)

For cDNA synthesis RT Kit was used with reaction mixture below:

Reaction:	1x (µl)
10x RT buffer	1.50
25x dNTPs (100 mM)	0.15
RNAse Inhibitors	0.10
RT Random primers	0.25
5x primer miR	1.50
H_2O (nuclease-free)	6.50
Reverse transcriptase (RT)	1.00
RNA (100 ng/µl)	1.00
total	15.0

Program for reaction was following:

Program:		
	16°C	30 min
	42°C	30 min
	85°C	5 min

After run of whole program 35 µl of nuclease-free water was added to reach the final amount of 50 µl.

qPCR – quantitative polymerase chain reaction

Mixture for qPCR reaction consisted of 2 fractions – DNA Master Mix and Primer Master Mix. Final volume of PCR reaction was 8 µl in total.

DNA Master Mix:	1x (µl)
TaqMan (Universal PCR Master Mix, cat. nr. 4324018)	2.0
H_2O (nuclease-free)	1.5
cDNA	0.5
total	4.0

Primer Master Mix:	1x (µl)
TaqMan (Universal PCR Master Mix, cat. nr. 4324018)	2.0
Primer (20 µM)	0.4
Probe (10 µM)	0.1
H_2O (nuclease-free)	1.5
total	4.0

miRNA Master Mix	1x (µl)
Taq	2.0
20x miR primer	0.4
H_2O (nuclease-free)	1.6
total	4.0

There were two separate mixtures for primers, one was for coding genes with specific probes for each gene; the other one for miRNA genes. Firstly 4 µl of Primer Master Mix were pipetted in 384 well plate, after that 4 µl of DNA Master Mix.

The reaction was performed by real time PCR instrument (HT7900, ABI) and with following program.

Program		
95°C	15 s	40 cycles
60°C	1 min	

4. Results

Leukemia and cancer development are highly connected to cell cycle and its pathways. Any slight change can have huge impact on future development of the cell (Vermeulen et al. 2003; Ghelli Luserna di Rorà et al. 2019). Small non-coding RNAs have much bigger impact on changing the expression of genes, than was earlier assumed. In this thesis we focused on studying the impact of miR-155 on two cell lines of Chronic Lymphocytic Leukemia. Workflow of experiments performed in thesis depicts **Chyba! Nenalezen zdroj odkazů.**

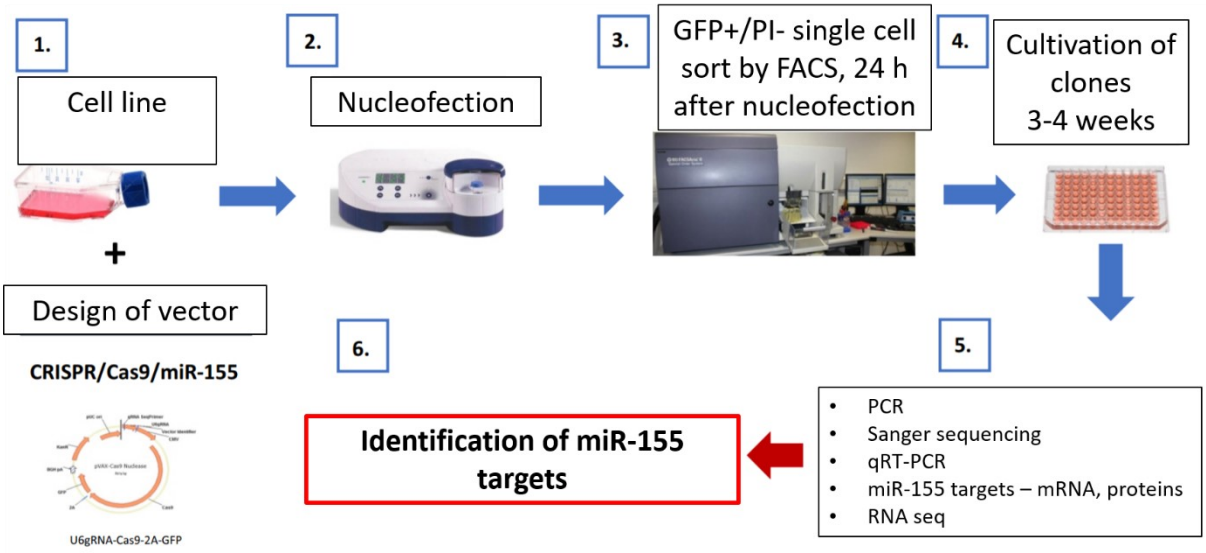

Fig. 8 Workflow of performed experiment. 1. Firstly there was cell line nucleofected with plasmid containing genes for CRISPR/Cas9 editing of miR-155. 2. Nucleofection was performed by AMAXA Nucleofector. 3. GFP+ and PI- cells were selected for further experiments by FACS. 4. Cultivation of selected clones lasted about 3-4 weeks, until gaining sufficient amount of cells for DNA and RNA isolation. 5. Experiments, such as PCR, Sanger sequencing – for confirmation of success rate in deleting of target region, qRT-PCR – for measuring the expression of target genes in gained clones and identifying the miR-155 targets were performed.

Here we focused on the leukemic HG-3 (shown in 9) and MEC-1 cell lines.

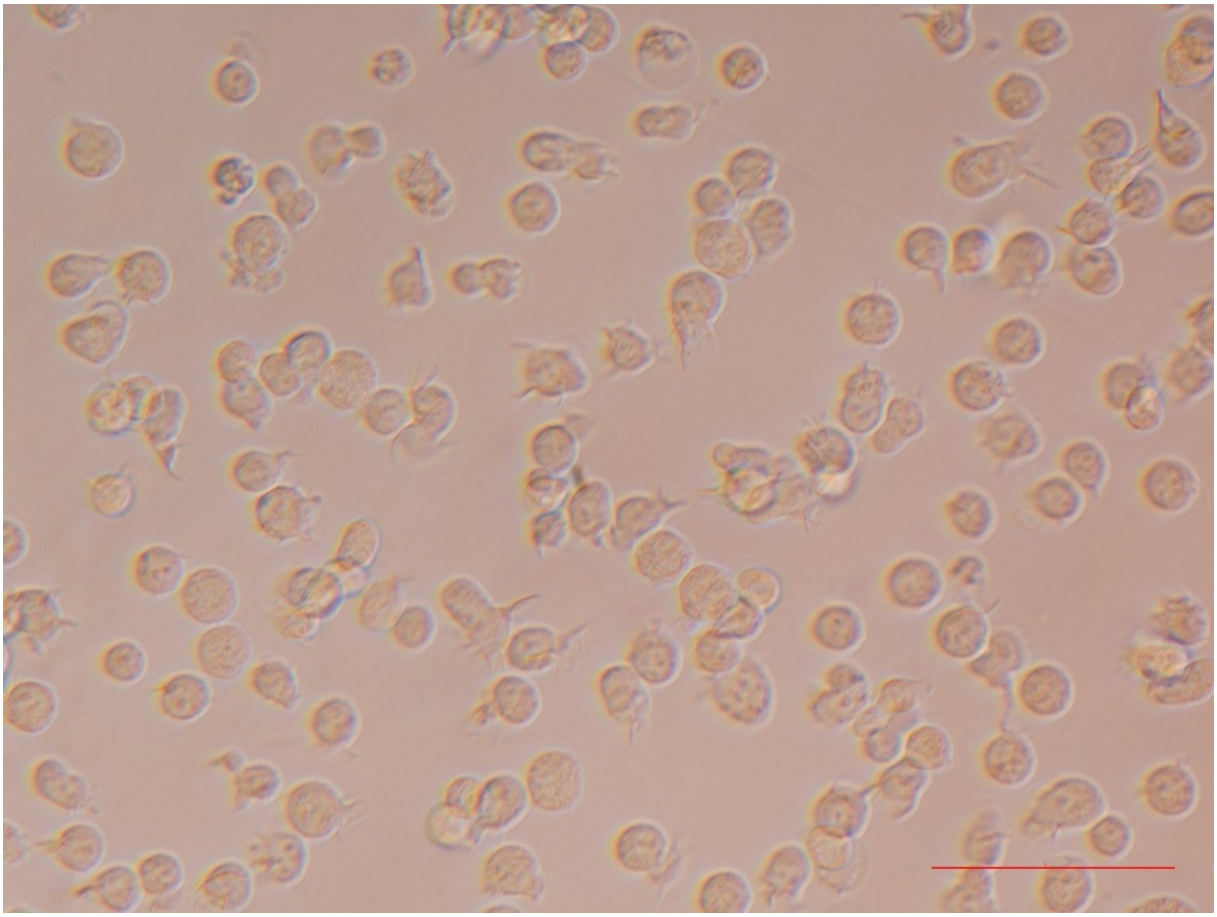

Fig. 9 HG-3 cell line (native). It is stable CLL cell line that consists of kvazi-mature B-cells growing in suspension. Magnification is 200x; one cell is around 5-10 μm large. The red line in the picture represents 25 μm.

Editing of the sequence coding for mature miR-155 by gene-editing technology CRISPR/Cas9 was performed in HG-3 cell line, which represents chronic lymphocytic leukemia (CLL) in early stage of progression. Editing of MEC-1 cell line was done in laboratory by others, in this thesis were perfomed experiments as cell count, cell viability and qRT-PCR. MEC-1 cells represents adverse CLL stage with *TP53* deletion (del17) (p11). For each gained clone of HG-3 cell line we performed separation of PCR product gel elektrophoresis followed by Sanger sequencing to check correctness of gene editing. Fig. 10 shows PCR product of single cell clones of HG-3 cell line, #4 is heterozygous with partial deletion in one strand, two bands are visible.

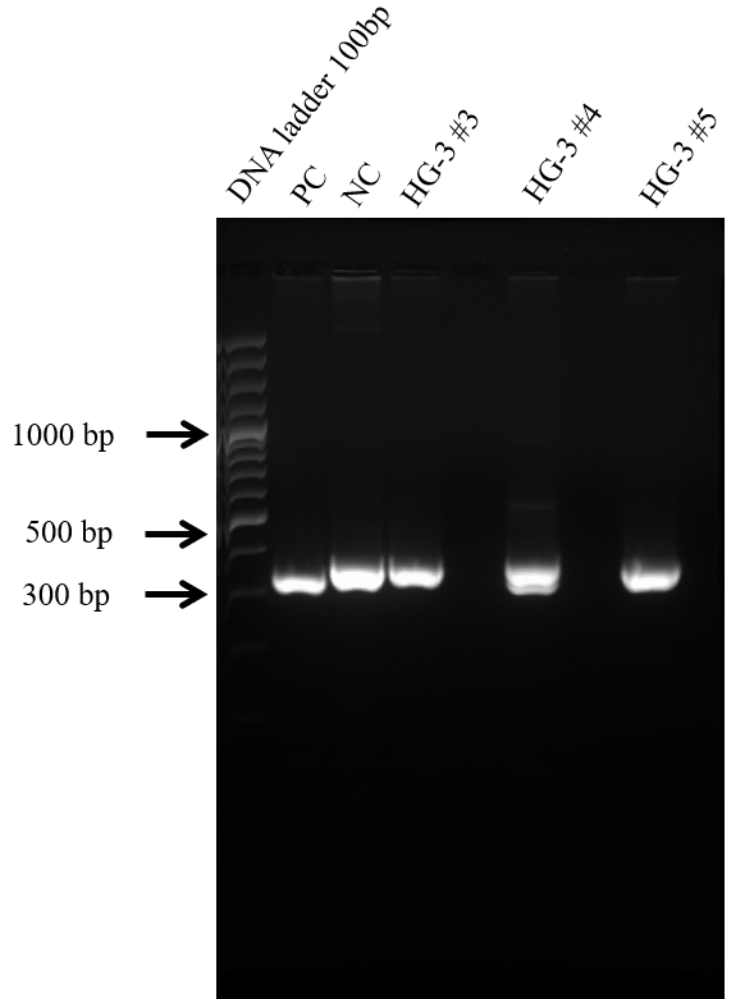

Fig. 10: PCR product of nucleofected HG-3 cell line with CRISPR/Cas9/miR-155 plasmid. Picture depicts different PCR product in CRISPR/Cas9/miR-155 clones isolated from HG-3 cell line. PCR product was separated on 2 % agarose gel, runned by 80 V/90 min. Size of PCR product of unedited miR-155 (ctrl) is 358 bp. First column contains DNA ladder 100 bp (#SM0323, ThermoScientific), second column represents positive control - clone #48 with biallelic deletion of miR-155 in MEC-1 cell line, third column represents negative control – wild type of HG-3 cell line (ctrl), fourth column represents clone #3 of HG-3 cell line, fifth column represents clone #4 of HG-3 cell line - containing changes in DNA sequence compared to wild type, two bands are visible, sixth column represents clone #5 of HG-3 cell line.

The model and effectivity of CRISPR/Cas 9 editing is shown in Fig. 11 and 12 for each cell line separately. Using the modern gene-editing technology CRISPR/Cas9 (Fig. 11B, C and D) we have successfully edited the sequence responsible for mature miR-155 at one genomic loci in HG-3 cells. This heterozygous clone #4 bears partially the deletion of the desired sequence, confirmed by Sanger sequencing of the PCR product (Fig. 11E). The same was performed with MEC-1 cell line, with the difference of gaining homozygous clone with deletion at both strands of DNA (Fig.11).

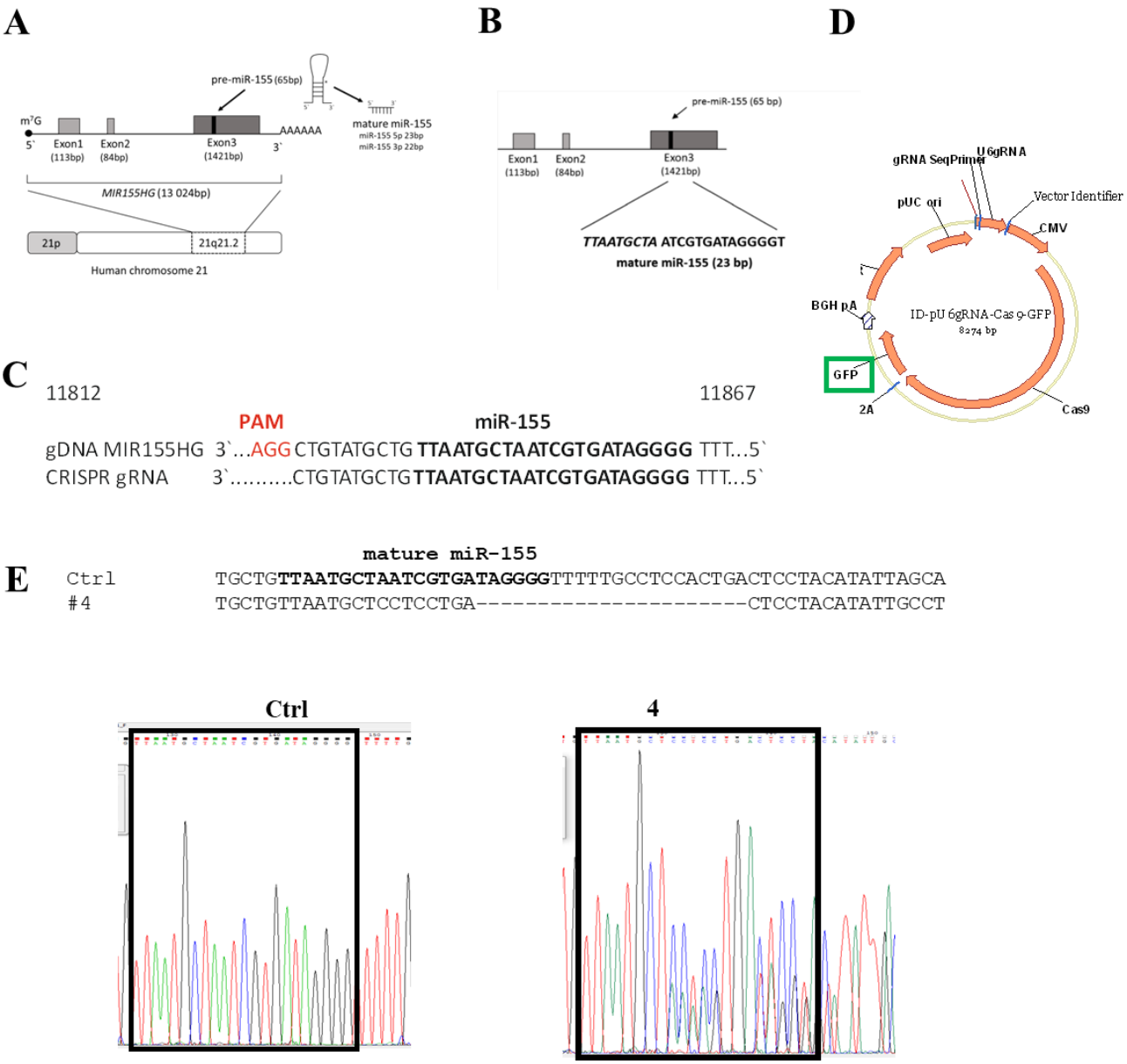

Fig. 11: Schematic illustration of *MIR155HG*, CRISPR/Cas9 miR-155 vector, and deletion of miR-155 in HG-3 cells. (A) Structure of the *MIR155HG/BIC* gene (NC_000021.8). *MIR155HG (BIC)* is localized on the 21q21.2 chromosomal locus. The full length of *MIR155HG* spans 13 024 bp that contains three exons. The exon 3 encodes precursor pre-miR-155 (1421 bp). After two endonuclease cleavage steps (by endonuclease Drosha and Dicer) arises the mature miR-155 (adapted and modified from Tam W, 2001,http://www.ncbi.nlm.nih.gov/gene/114614). **(B)** Scheme of *MIR155HG/BIC* gene with depicted and highlighted sequence for mature miR-155 (23 bp). **(C)** The sequence of *MIR155HG* coding mature miR-155 (in bold) and target sequence for gRNA. The PAM sequence AGG in red color. **(D)** Scheme of CRISPR/Cas9/miR-155 vector (pU6gRNA-Cas9-GFP, 8274 bp, Sigma). The vector contains Kanamycin resistance, the sequence for green fluorescence protein (GFP) used as a selection mark. **(E)** The scheme shows the region of *MIR155HG* from 5` 11819 to 11879 3` end, where 21 nt are deleted in case of HG-3 miR-155 deficient clone #4 (heterozygous mutation) in comparison to ctrl (non-edited HG-3 cells). Seed sequence is TAATGCTA. The lower part of the picture shows chromatograms (Sanger sequencing, Chromas software for visualization of pictures were used) of the PCR product in HG-3 cells (ctrl vs #4).

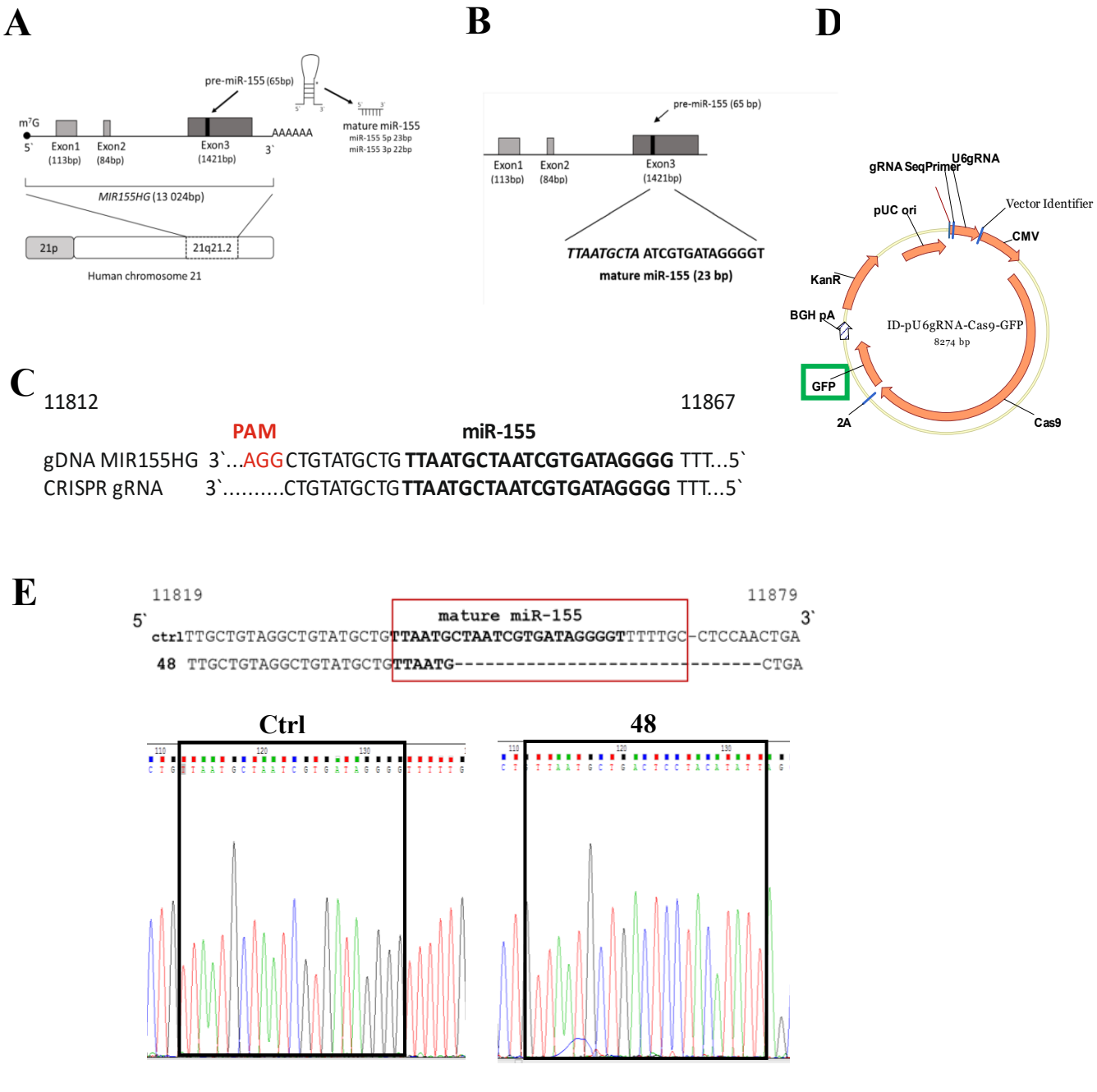

Fig. 12: Schematic illustration of *MIR155HG*, CRISPR/Cas9 miR-155 vector, and deletion of miR-155 in MEC-1 cells. (A) Structure of the *MIR155HG/BIC* gene (NC_000021.8). *MIR155HG (BIC)* is localized on the 21q21.2 chromosomal locus. The full length of *MIR155HG* spans 13 024 bp that contains three exons. The exon 3 encodes precursor pre-miR-155 (1421 bp). After two endonuclease cleavage steps (by endonuclease Drosha and Dicer) arises the mature miR-155 (adapted and modified from Tam W, 2001,http://www.ncbi.nlm.nih.gov/gene/114614). **(B)** Scheme of *MIR155HG/BIC* gene with depicted and highlighted sequence for mature miR-155 (23 bp). **(C)** The sequence of *MIR155HG* coding mature miR-155 (in bold) and target sequence for gRNA. The PAM sequence AGG in red color. **(D)** Scheme of CRISPR/Cas9/miR-155 vector (pU6gRNA-Cas9-GFP, 8274 bp, Sigma). The vector contains Kanamycin resistance, the sequence for green fluorescence protein (GFP) used as a selection mark. (**E)** The scheme shows the region of *MIR155HG* from 5‘ 11819 to 11879 3‘ end, where 21 nt are deleted in case of MEC-1 miR-155 deficient clone #48 (homozygous mutation) in comparison to ctrl (non-edited MEC-1 cells). Seed sequence is TAATGCTA. The lower part of the picture shows chromatograms (Sanger sequencing, Chromas software for visualization of pictures were used) of the PCR product in MEC-1 cells (ctrl vs #48).

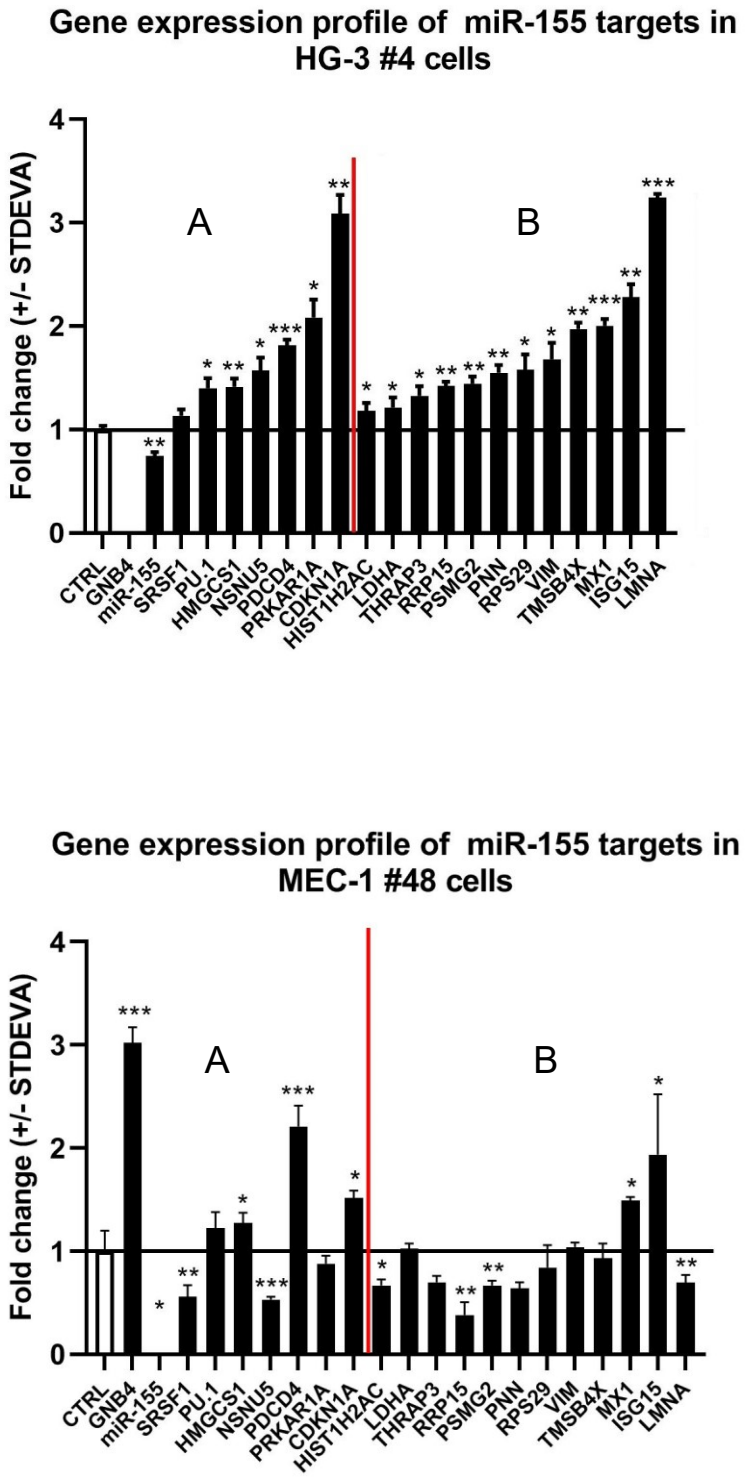

Fig. 13: Gene expression profile of miR-155 targets (validated, novel bona fide CLL related) in HG-3 and MEC-1 cell lines. Graph on the upper part of the figure shows data from HG-3 cell line, knock-out in one DNA strand *hsa-miR-155* gene. Graph on the bottom shows data from MEC-1, knock-out on both DNA strands of *hsa-miR-155* gene. Ct values of experimental genes were normalized to the reference gene *GAPDH*. The expression of mRNAs was determined by TaqMan chemistry. **A** Confirmed (based on miRtarBase database) miR-155 targets are in left part of the graph, **B** Novel, and bona fide CLL related miR-155 targets are behind the red line. Data are from 2 independent experiments. Ctrl (gene expression of cells without gene editing) was set to 1. Statistics t-test, two tailed, unpaired was used (* $p<0.05$; ** $p<0.005$, *** $p<0,0005$).

Fig. 13 depicts results of qPCR measurement. In part, which is labeled “A” in first column is wild type (unedited cell line) of each cell line set at 1 as a control, the expression of other genes is normalized to this value. Following genes (selection of genes was done based on mRNAseq data of MEC-1 cell line) are validated targets of miR-155: *GNB4* - G Protein Subunit Beta 4 gene is located in plasma membrane, coding G protein subunit. *SRSF1* - Serine And Arginine Rich Splicing Factor 1 protein is located in nucleus and is part of alternative splicing.

PU.1- Transcription factor PU.1, located in nucleus which binds to a purine-rich DNA sequence, can act as lymphoid-specific enhancer, this protein is specifically involved in activation and differentiation of macrophages and B-cells. *HMGCS1*-Hydroxymethylglutaryl-CoA synthase is an enzyme, located in cytosol and nucleus, catalysing condensation of acetyl-CoA with acetoacetyl-CoA. *NSNU5* - NOP2/Sun RNA Methyltransferase 5 codes a protein located in nucleus, member of conserved family of methyltransferases. *PDCD4* – coding gene of Programmed Cell Death 4, which is located in nucleus and cytosol, works as tumor suppressor. PRKAR1A - Protein Kinase cAMP-Dependent Type I Regulatory Subunit Alpha, located in plasma membrane and cytosol.

CDKN1A - Cyclin Dependent Kinase Inhibitor 1A is in nucleus and cytosol. This gene encodes a potent cyclin-dependent kinase inhibitor. This specific inhibitor binds to cyclin-cyclin-dependent kinase 2 or 4 complexes, therefore works as regulator of cell cycle in G1 phase. Expression of this gene is regulated by p53, suppressor protein and can stop the proliferation of cell. In part “B” of the Figure 13 are genes, which are potential targets of miR-155 associated with CLL. *HIST1H2AC* - Histone H2A type 1-C, this protein is located solely in nucleus, part of nucleosomal octamer.

LDHA - Lactate Dehydrogenase A is located in extracellular compartment, cytosol and nucleus. This protein catalyzes the metabolic pathway – converting of L-lactate and NAD to pyruvate and NADH, as last step of anaerobic glycolysis. This protein is more expressed in cancer and leukemic diseases in order to avoid using mitochondria and cellular respiration cycle as source of energy. *THRAP 3* - Thyroid Hormone Receptor Associated Protein 3, located in nucleus and extracellular compartment, this protein is involved in pre-mRNA splicing.

RRP15 - Ribosomal RNA Processing 15 Homolog, located in nucleus, part of protein maturation processes. *PSMG2* - Proteasome Assembly Chaperone 2, located in nucleus, plasma, membrane and cytoskeleton, one of chaperone proteins, part of assembly of 20S proteasome.

PNN - Pinin, Desmosome Associated Protein, located in nucleus, plasma membrane and cytoskeleton, transcriptional activator of the E-cadherin promoter gene. *RPS29* – Ribosomal Protein S29, located in cytosol, extracellular compartment, nucleus, endoplasmic reticulum, this protein is component of the 40S subunit of ribosomal proteins. *VIM* – Vimentin, located in extracellular compartment, cytoskeleton, peroxisome and cytosol, part of intermediate filament protein.

TMSB4X - Thymosin Beta 4 X-Linked, located in cytoskeleton, nucleus and cytosol, actin sequestering protein, plays a role in actin polymerization, this protein is also involved in cell proliferation, migration and differentiation.

MX1 - MX Dynamin Like GTPase 1, located in nucleus and cytosol, this gene encodes protein, which participated in the cellular antiviral response. *ISG15* - ISG15 Ubiquitin Like Modifier, located in extracelular compartment, nucleus and cytosol, this protein functions similarly as ubiquitin.

LMNA - Lamin A/C, located in cytoskeleton, nucleus, cytosol, this protein is part of cytoskeletal proteins.

GNB4 differently expressed in HG-3 as in MEC-1.

As the cells of miR-155 deficient clones (originating from the single cell) were proliferating slower compared to unedited cells during routine cell culturing, we have decided to follow these observations with advanced approaches. Firstly, we did the standard cell count to assess the cell growth and plot the proliferation curve for both HG-3 and MEC-1 cells (Fig. 13 and 14).

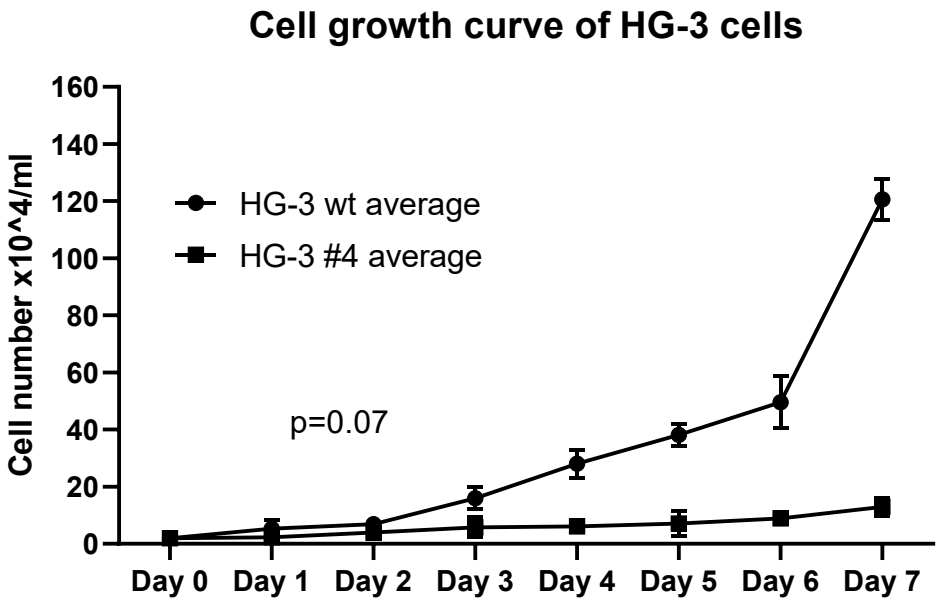

Fig. 14: The proliferation rate of human CLL cell line HG-3. Cell growth curve of HG-3 cells (ctrl - wt and miR-155 deficient clone #4) was determined by cell number count by hemocytometer within 7 days. Seeding density at day 0 was 20 000 cells per well. Y-axis shows cell number and X-axis day. Data represent the mean of 2 independent experiments (+/-STDEVA). Statistics: t-test, two tailed, unpaired was used, p>0.05.

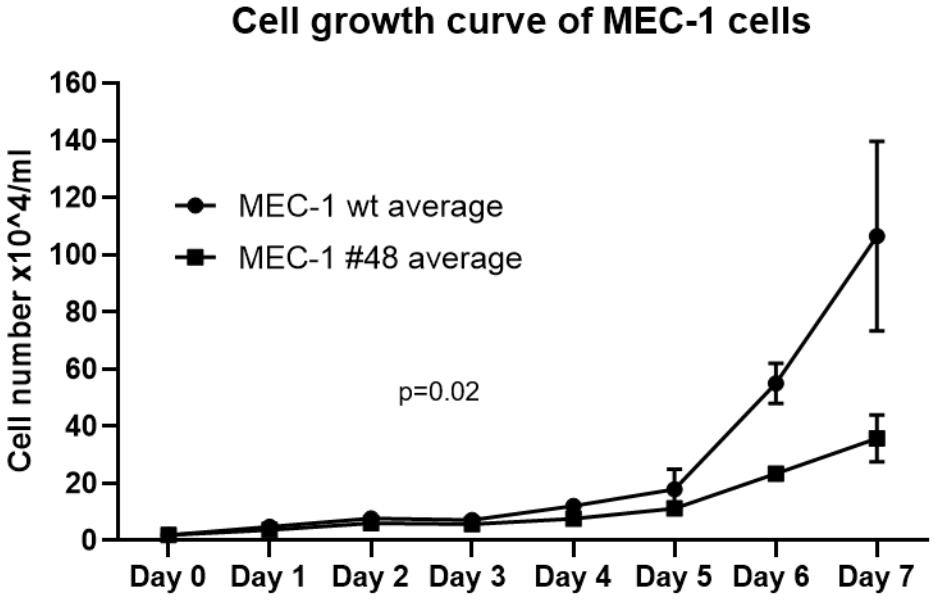

Fig. 15: The proliferation rate of human CLL cell line MEC-1. Cell growth curve of MEC-1 cells (ctrl - wt and miR-155 deficient clone #48) was determined by cell number count by hemocytometer within 7 days. Seeding density at day 0 was 20 000 cells per well. Y-axis shows cell number and X-axis day. Data represent the mean of 2 independent experiments (+/-STDEVA). Statistics: t-test, two tailed, unpaired was used, p>0.05.

In both cell growth curves is significantly visible difference in the level of proliferation speed between wild-type cells and edited clones.

According to this finding, we were curious, if the slower cell growth is connected to higher occurrence of apoptosis or not. Therefore we performed flow cytometry measurement of cells stained with apoptotic protein Annexin V (APC) in period of 7 days. Population of dead cells was detected by propidium iodide. All measurements by flow cytometry are shown in Fig. 16 and 17.

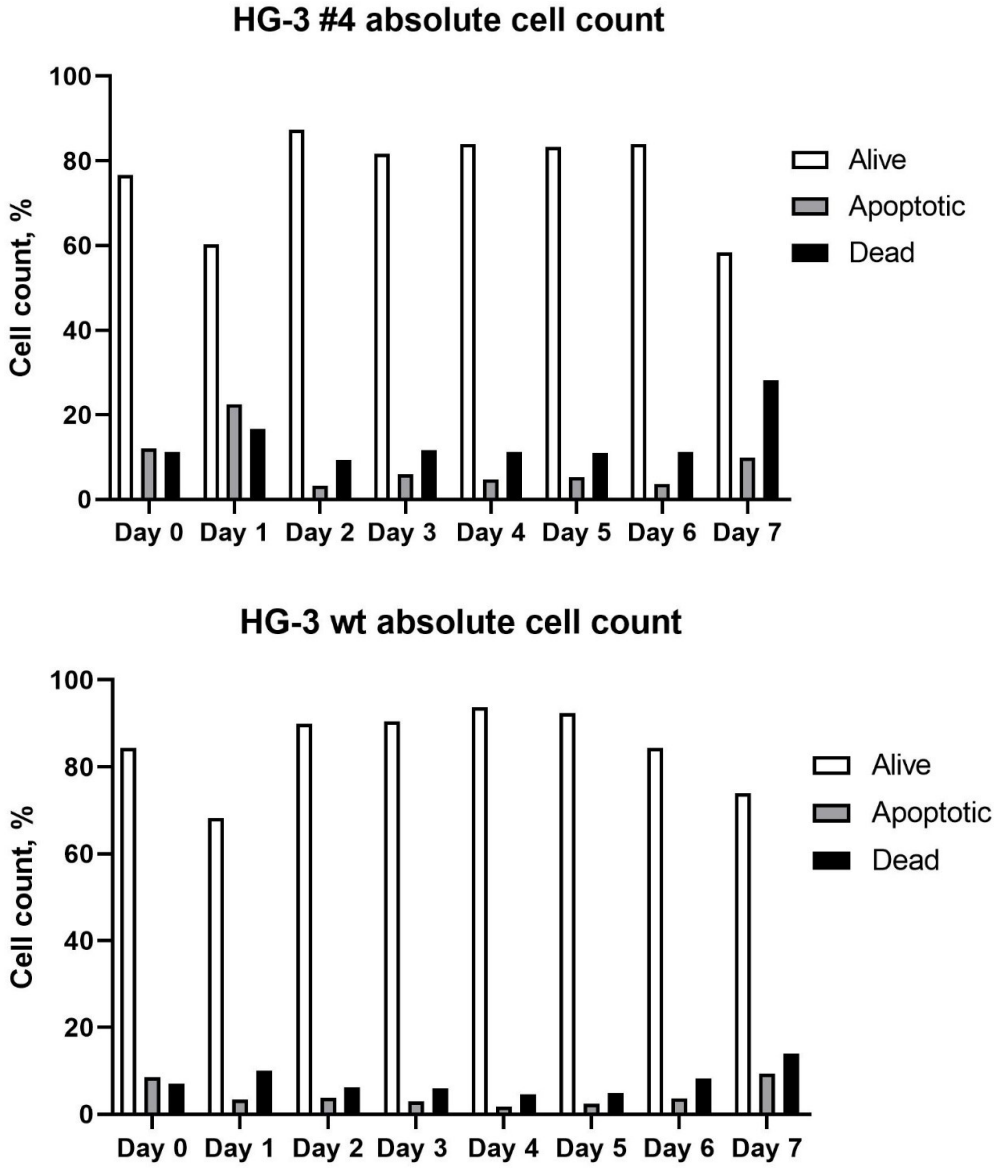

Fig. 16: Viability of HG-3 cells (Evaluation of apoptosis by flow cytometry. HG-3 cells (ctrl and miR-155 deficient clone #4) were stained by *Annexin V/PI* (X-axis, Annexin V, APC, and Y-axis, PI in PE-Cy7 channel). Data were evaluated by Diva software and the measurement was performed with the use of the FACS Canto II BD flow cytometer.

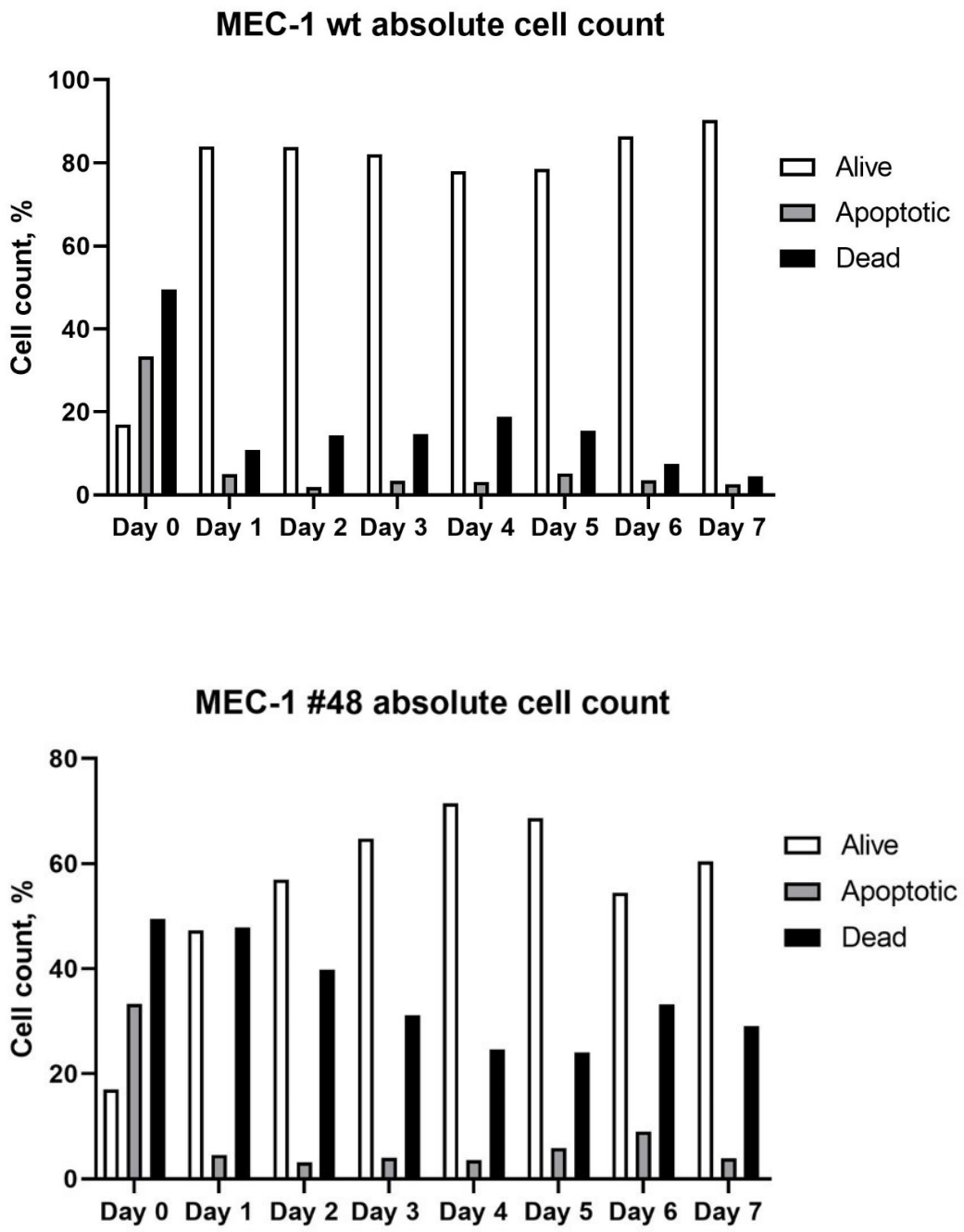

Fig. 17: Viability of MEC-1 cells (Evaluation of apoptosis by flow cytometry. MEC-1 cells (ctrl and miR-155 deficient clone #48) were stained by *Annexin V/PI* (X-axis, Annexin V, APC, and Y-axis, PI in PE-Cy7 channel). Data were evaluated by Diva software and the measurement was performed with the use of the FACS Canto II BD flow cytometer.

As shows Fig. 16 there is practically no difference in the population of apoptotic and dead cells in HG-3 cell line wt vs edited clone #4. Interestingly, MEC-1 cell line shows higher abundance population of dead cells in edited clone #48 in comparison to wild type MEC-1.

5. Discussion

We worked with two CLL cell lines, both of them with higher expression of miR-155 in comparison to the normal healthy B-cells. HG-3 cell line shows lower expression than MEC-1 that is in concordance with the level of disease stage. We performed nucleofection of these cell lines with plasmid containing all sequences for CRISPR/Cas9 system, gRNA and GFP for detection (for details see Fig.11 D). Gene editing of MEC-1 cell line was performed formerly by Dr. Savvulidi Vargová and the system of gaining mutant cell line remained the same.

1. By CRISPR/Cas9 tool we created deletion mutant of human B-CLL cell line HG-3 that do not express miR-155.

We provided insertion of plasmid by nucleofection, which is electroporation-based transfection method enabling transfer of nucleic acids such as DNA or RNA into cells by applying a specific voltage and reagents. The survival rate of B-cells after nucleofection and flow cytometer cell sorting is generally quite low (Seiffert et al., 2007); we achieved about 1,4 % of cell survival, gaining one clone with changes in DNA sequence. The deletion of miR-155 was partially successful as we gained a clone with deletion of six nucleotides in the coding region of miR-155, positioned on one strand of DNA, therefore heterozygous clone. We assume, that this low effect is also caused by the low level of progression of CLL in HG-3 cells (intermediate state of CLL), compared to MEC-1 cell line, where the success rate in nucleofection and changing the DNA by CRISPR/Cas9 method was higher (4,3 %). Also according to Dr. Seiffert, the larger the nucleofected plasmid is, the higher rate of apoptosis occurs. In our experiments we observed apoptotic rate around 10 % in both CLL cell lines. To avoid technical difficulties, changing of the delivery method may be considered, by lentivirus for example (García-Tuñón et al., 2017).

In order to identify which nucleotides were deleted by CRISPR/Cas9 we performed Sanger sequencing of PCR product, which showed the deletion in one strand clearly, in the second strand were some changes, but not so clearly identifiable. We would suggest in case of gaining more clones and choosing the best for further studies, to perform subcloning of PCR product into E.coli cells in order to confirm the best fortunate clone.

2. Explore the impact of miR-155 deletion on HG-3 cell line viability and proliferation.

Even though the deletion in HG-3 cell line was just partial in coding sequence of miR-155 and executed in one strand of DNA, the cell growth curve shows, that the number of cells grew with difference between wild type and heterozygous clone. Our results provide support for our research hypothesis. P-value comes up to 0.07, therefore we can't reject the null hypothesis, but the cell growth curve grows significantly higher in seventh day, which is the last day of measurment. If we provided the measurment for longer time, maybe we would record lower p-value. On the other hand, cell growth curve of MEC-1 cell line, has significant difference, as a result we can confirm, that changes in the DNA sequence of miR-155, and deletion of nucleotides lead to slower proliferation of MEC-1 cell line.

Cell viability

We made measurment of viability of both cell lines during 7 days by flow cytometry, focusing on the number of alive, apoptotic and dead cells (Fig. 8, 9). Cells were stained by *Annexin V/PI*. The number of HG-3 cells was stable throughout the seven days, about 80 % of cells was alive, the number started to change at the seventh day, any actual difference between control (wild type) and miR-155 heterozygous clone was not detected. These graphs support the data from cell growth curve, that during first six days the number of cells doesn't change much. This can be explained by the moderate level of CLL progression.

MEC-1 cell line showed different outcome, wild type shows high number of alive cells throughout the seven days, quite interestingly, the percentage of alive cells is growing after fifth day. The results from Day 0 we don't include in the observation, because of some propably technical difficulties, since the same trend occurs in both wild type and clone. MEC-1 homozygous clone shows different ratio of alive and dead cells, it may be caused by higher assumption to die because of genetic changes – thanks to CLL, and „curing" by lack of miR-155, which blocks dying of cells. Or, according to data from the beginning of measurement (Days 1-3), it can be caused by defrosting of wrong cryotube with already high amount of dead cells.

Conclusion of these viability measurments is, that in HG-3 cell line, the viability actually didn't change. In MEC-1 cell line there are changes, but not provided with enough evidence and many factors, which can cause the difference, without any significant influence of the

deleting of miR-155. Therefore it would be appropriate to perform this experiment again to distinguish what caused the difference.

3. Comparison of the gene expression profile of HG-3 cells before and after gene editing.

We performed qRT-PCR for both CLL cell lines, as show Fig. 13. We aligned genes by its expression. Expression of these genes in wild type was set as control to the value 1 and other genes were compared to this relative value. Genes were aligned by ct value, firstly validated targets, in part „A“, in part „B“ are shown genes which may be bona fide targets of miR-155 in CLL.

The most visible difference between HG-3 and MEC-1 cell line is the expression of *GNB4* gene, in HG-3 there wasn't any measurable value, on the other hand in MEC-1, its expression was significantly higher, therefore we can confirm *GNB4* as miR-155 target. In comparison, the *GNB4* may be part of different pathway in cancerogenesis, according to its overexpression in breast cancer cells (B. Wang et al., 2018). The difference in these CLL cell lines may be caused by the progressive state of the disease, but presumably the reason may be the level of miR-155 expression. As we can see right away at the third column, the expression of miR-155 in HG-3 is lower, than wild type, but not distinctively.

Further expressed gene is *hsa-miR-155*, as mentioned above, clearly deletion of 6 nucleotides within the mature sequence of miR-155 located on one DNA strand, is not sufficient for complete loss of its function. In MEC-1 cell line this deletion was successful, we gained biallelic deletion (homozygous clone), therefore comparison of miR-155 expression in clone #48 versus wild type cells is more reliable in MEC-1 cell line than in HG-3 cells.

The expression of *SRSF1* is in HG-3 heterozygous clone slightly higher, than in control and significantly lower in MEC-1 homozygous clone, which means, that in CLL this gene is likely upregulated by miR-155. Protein encoded by *SRSF1* is involved in RNA processing.

SP1 gene, in Fig. 13 named as *PU.1*, encodes PU.1 transcription factor. As it is direct and validated target of miR-155, we supposed its upregulation (in different rate based on deletion level of miR-155) in both cell lines after gene editing. PU.1 is confirmed target of miR-155 in CLL cells (Huskova et al., 2015; Vargova K et al, 2011 and 2017). Interestingly, expression of PU.1 was 0.5 fold in both cell lines after gene editing. This fact could be explained by

existence of some compensation molecule, secondary target of miR-155 that could regulate PU.1 expression in CLL cells.

HMGCS1 expression is in HG-3 heterozygous clone and MEC-1 homozygous clone slightly higher, than in wild type. This gene encodes catalytical protein Hydroxymethylglutaryl-CoA synthase.

The expression of *NSUN5* is in HG-3 heterozygous clone higher, than in control and significantly lower in MEC-1 homozygous clone, which means, that in CLL this gene is usually upregulated by miR-155. *NSUN5* encodes a methyltransferase, which can effect expression of genes.

PDCD4 gene is associated with apoptosis, encodes Programmed Cell Death 4 protein, which inhibits translation initiation and acts as tumor supressor. Therefore it's not surprising, that in both HG-3 and MEC-1 cell line this gene is extremely supressed in CLL wild type, more in MEC-1 respectively.

PRKAR1A encodes regulatory subunit of the cAMP-dependent protein kinases. Its expression differs in HG-3 heterozygous clone, where it's two fold higher, than in wild type, and it's expression is slightly lower in MEC-1 homozygous clone.

CDKN1A encodes a potent cyclin-dependent kinase inhibitor, which binds to complexes of cyclin-cyclin-dependant kinase 2 and 4, by this activity it prevents continuing of cell cycle to S phase. In HG-3 cell line is this gene

„Not- validated targets" a bona fide targets of miR-155 in CLL cells

HIST1H2AC encodes Histone H2A type 1-C protein, which is part of nucleosome, its expression in heterozygous clone of HG-3 cell line, is slightly over the control and in MEC-1 cell line the expression decreased.

LDHA is another gene of catalytical protein, Lactate Dehydrogenase A, this enzyme catalyzes the conversion of L-lactate and NAD to pyruvate and NADH during anaerobic glycolysis. Physiological expression of this protein is higher in oxygen-poor environment. Otherwise, even in oxygen-rich environment, this enzyme is highly expressed in cancer cells (Arseneault et al., 2013). Therefore we expected higher expression of *LDHA* in unedited HG-3 and MEC-1 cell lines. Surprisingly, based on our results, the expression of *LDHA* was in

both cell lines about control level. Therefore we could assume, that this protein is not affected by miR-155 expression in CLL cells.

THRAP3 encodes protein, which is involved in pre-mRNA splicing and can trigger mRNA decay. This gene is more expressed in heterozygous clone of HG-3 cell line than in wild type, on the other hand, in MEC-1 cell line homozygous clone it's downregulated. This difference could indicate to changes in mRNA splicing due to different expression of miR-155 in edited CLL cells.

RRP15's level of expression in HG-3 clone is about 0.5 fold, in MEC-1 clone this gene is about of control's level of expression, which means, that normally is this gene in CLL cell line upregulated due to miR-155 overexpression.

PSMG2 encodes a chaperone protein. In HG-3 clone this gene is upregulated, on the other hand in MEC-1 clone downregulated. Again, we could assume that this difference is due to different miR-155 expression in edited CLL cells.

VIM encodes protein Vimentin, which is part of cytoskeletal intermediate filaments. Its expression is upregulated in HG-3 heterozygous clone, but at the same level as wild type in MEC-1 cell line.

TMSB4X is also gene encoding protein connected to cytoseleton, but as part of actin-associated proteins. In HG-3 cell line clone it's two times upregulated, in MEC-1 the level of expression is at the same level as wild type.

MX1 gene (Interferon-induced GTP-binding protein) is 0.5 - 1.0 fold upregulated in both HG-3 and MEC-1 cell line.

ISG15 encodes ubiquitin-like protein, which conjugates to intracellular target proteins. It has also function of chemotactic activity towards neutrophils. This gene is upregulated (1.0-1.5 fold) in both clones.

LMNA shows also surprising level of expressions. In HG-3 cell line the level is highest which was measured within all genes (2 fold), on the other hand in MEC-1 cell line the expression is lower, but close to wild type level. *LMNA* encodes Lamin, which is also part of cytoskeleton proteins group.

We performed qPCR of 20 different genes, beside *hsa-miR-155*, all of them with different function, but some of them can be separated into small groups according based on their function. Some results gained from HG-3 heterozygous clone are in correlation with the level of expression of same genes in MEC-1 cell line, but some differ showing also quite the opposite. Because of these results and also expression of *hsa-miR-155* gene, which was supposed to be downregulated, ideally to minimum, the results shouldn't be taken that strong.

If we look at expression of some groups, we may find some interesting results, for example the level of expression of cytoskeleton connected group that consists of *PNN, VIM, LMNA* and *TMSB4X*. If we just focus on results measured in MEC-1 cell line (reason mentioned above), we may see that the level of expression in homozygous clone is mostly the same as wild type expression level, or slightly decreased, which means, that *hsa-miR-155* doesn't affect their expression. Because also these genes are in group of not-confirmed targets, these results support that they are not targets. On the website rnacentral.org is *VIM* listed as target of *hsa-miR-155*, verified by microarrays. But our results show the opposite.

In group of catalytical proteins we have *HMGCS1* - validated target and *LDHA* – not validated target. According to our measurment *HMGCS1* is affected by miR-155 expression, but the level of *LDHA* is the same as control, therefore we assume that it's not a target of *hsa-miR-155* in CLL cells.

PDCD4 and *CDKN1A* are genes connected to cell cycle or apoptosis, both of them are validated targets of miR-155, which is also supported by our results.

To answer the specific aims of the thesis:

We detected differences in the transcriptom of both cell lines, in HG-3 those were mostly higher expressions of both, novel and validated targets, which seems to be misleading, according not complete, or successful deletion of *hsa-miR-155* in this cell line. In MEC-1 cell line we observed both up and down regulations, most of validated targets were upregulated. In the group of novel or potential targets there were two genes upregulated (*TMSB4X, MX1*), but most of them showed no changes in expression or just slightly lower, than control. Those which were at the same level as control are probably not targets of *hsa-miR-155.*

Even though the results of gene expression in HG-3 cell line were not strong enough for deciphering which genes are targets of *hsa-miR-155*, the incomplete deletion within its

sequence impairs cell growth observed in period of one week. Simmilar results were achieved with MEC-1 cell line, in miR-155 deficient clone #48.

All the information according to gene coding and function of proteins were taken from genecards.org, list of validated targets was found on rnacentral.org website.

6. Conclusion

In this thesis we performer CRISPR/Cas9 gene editing of *hsa-miR-155* in HG-3 cell line, which lead to gaining heterozygous clone. Later we executed Further experiments, such as measurement of the cell proliferation and viability of HG-3 and MEC-1 cell lines. We gained different levels of expressed target genes of *hsa-miR-155* by qRT-PCR in both of these cell lines, and homozygous and heterozygous clones.

7. List of Abbreviations

CDKN1A	Cyclin Dependent Kinase Inhibitor 1A
CLL	chronic lymphocytic leukemia
DMSO	dimethylsulfoxi
FACS	fluorescence activated cell sorting
FBS	fetal bovine serum
FCR	combination of drugs: fludarabine, cyclophosphamide, rituximab
GNB4	G Protein Subunit Beta 4
HIST1H2AC	Histone H2A type 1-C
HMGCS1	Hydroxymethylglutaryl-CoA synthase
ISG15	ISG15 Ubiquitin Like Modifier
LDHA	Lactate Dehydrogenase A
LMNA	Lamin A/C
miR-155	microRNA - 155
MX1	MX Dynamin Like GTPase 1
NSNU5	NOP2/Sun RNA Methyltransferase 5
PBS	phosphate buffered saline
PDCD4	Programmed Cell Death 4
PNN	Pinin, Desmosome Associated Protein
PRKAR1A	Protein Kinase CAMP-Dependent Type I Regulatory Subunit Alpha
PSMG2	Proteasome Assembly Chaperone 2
PU.1	Transcription factor PU.1
qPCR	quantitative polymerase chain reaction
RPS29	Ribosomal Protein S29

RRP15	Ribosomal RNA Processing 15 Homolog
SRSF1	Serine And Arginine Rich Splicing Factor 1
THRAP 3	Thyroid Hormone Receptor Associated Protein 3
TMSB4X	Thymosin Beta 4 X-Linked
VIM	Vimentin

8. References

Almeida, M. I., Reis, R. M., & Calin, G. A. (2011). MicroRNA history: Discovery, recent applications, and next frontiers. *Mutation Research/Fundamental and Molecular Mechanisms of Mutagenesis*, *717*(1), 1–8. https://doi.org/10.1016/j.mrfmmm.2011.03.009

Arseneault, R., Chien, A., Newington, J. T., Rappon, T., Harris, R., & Cumming, R. C. (2013). Attenuation of LDHA expression in cancer cells leads to redox-dependent alterations in cytoskeletal structure and cell migration. *Cancer Letters*, *338*(2), 255–266. https://doi.org/10.1016/j.canlet.2013.03.034

Babar, I. A., Cheng, C. J., Booth, C. J., Liang, X., Weidhaas, J. B., Saltzman, W. M., & Slack, F. J. (2012). Nanoparticle-based therapy in an in vivo microRNA-155 (miR-155)-dependent mouse model of lymphoma. *Proceedings of the National Academy of Sciences of the United States of America*, *109*(26), E1695-1704. https://doi.org/10.1073/pnas.1201516109

Barrangou, R., Fremaux, C., Deveau, H., Richards, M., Boyaval, P., Moineau, S., Romero, D. A., & Horvath, P. (2007). CRISPR Provides Acquired Resistance Against Viruses in Prokaryotes. *Science*, *315*(5819), 1709–1712. https://doi.org/10.1126/science.1138140

Barrangou, Rodolphe. (2015). Diversity of CRISPR-Cas immune systems and molecular machines. *Genome Biology*, *16*(1), 247. https://doi.org/10.1186/s13059-015-0816-9

Carthew, R. W., & Sontheimer, E. J. (2009). Origins and Mechanisms of miRNAs and siRNAs. *Cell*, *136*(4), 642–655. https://doi.org/10.1016/j.cell.2009.01.035

Costinean, S., Zanesi, N., Pekarsky, Y., Tili, E., Volinia, S., Heerema, N., & Croce, C. M. (2006). Pre-B cell proliferation and lymphoblastic leukemia/high-grade lymphoma in E -miR155 transgenic mice. *Proceedings of the National Academy of Sciences*, *103*(18), 7024–7029. https://doi.org/10.1073/pnas.0602266103

DeKoter, R. P., & Singh, H. (2000). Regulation of B lymphocyte and macrophage development by graded expression of PU.1. *Science (New York, N.Y.)*, *288*(5470), 1439–1441. https://doi.org/10.1126/science.288.5470.1439

Deltcheva, E., Chylinski, K., Sharma, C. M., Gonzales, K., Chao, Y., Pirzada, Z. A., Eckert, M. R., Vogel, J., & Charpentier, E. (2011). CRISPR RNA maturation by trans-

encoded small RNA and host factor RNase III. *Nature*, *471*(7340), 602–607. https://doi.org/10.1038/nature09886

Eis, P. S., Tam, W., Sun, L., Chadburn, A., Li, Z., Gomez, M. F., Lund, E., & Dahlberg, J. E. (2005). Accumulation of miR-155 and BIC RNA in human B cell lymphomas. *Proceedings of the National Academy of Sciences of the United States of America*, *102*(10), 3627–3632. https://doi.org/10.1073/pnas.0500613102

Emerging Role of CRISPR/Cas9 Technology for MicroRNAs Editing in Cancer Research | Cancer Research. (b.r.). Získáno 23. prosinec 2020, z https://cancerres.aacrjournals.org/content/77/24/6812.short

Fabbri, M., & Croce, C. M. (2011). Role of microRNAs in lymphoid biology and disease. *Current Opinion in Hematology*, *18*(4), 266–272. PubMed. https://doi.org/10.1097/MOH.0b013e3283476012

Friedland, A. E., Tzur, Y. B., Esvelt, K. M., Colaiácovo, M. P., Church, G. M., & Calarco, J. A. (2013). Heritable genome editing in C. elegans via a CRISPR-Cas9 system. *Nature Methods*, *10*(8), 741–743. https://doi.org/10.1038/nmeth.2532

Fu, Y., Sander, J. D., Reyon, D., Cascio, V. M., & Joung, J. K. (2014). Improving CRISPR-Cas nuclease specificity using truncated guide RNAs. *Nature Biotechnology*, *32*(3), 279–284. https://doi.org/10.1038/nbt.2808

García-Tuñón, I., Hernández-Sánchez, M., Ordoñez, J. L., Alonso-Pérez, V., Álamo-Quijada, M., Benito, R., Guerrero, C., Hernández-Rivas, J. M., & Sánchez-Martín, M. (2017). The CRISPR/Cas9 system efficiently reverts the tumorigenic ability of BCR/ABL in vitro and in a xenograft model of chronic myeloid leukemia. *Oncotarget*, *8*(16), 26027–26040. https://doi.org/10.18632/oncotarget.15215

Garneau, J. E., Dupuis, M.-È., Villion, M., Romero, D. A., Barrangou, R., Boyaval, P., Fremaux, C., Horvath, P., Magadán, A. H., & Moineau, S. (2010). The CRISPR/Cas bacterial immune system cleaves bacteriophage and plasmid DNA. *Nature*, *468*(7320), 67–71. https://doi.org/10.1038/nature09523

Georgantas, R. W., Hildreth, R., Morisot, S., Alder, J., Liu, C., Heimfeld, S., Calin, G. A., Croce, C. M., & Civin, C. I. (2007). CD34+ hematopoietic stem-progenitor cell microRNA expression and function: A circuit diagram of differentiation control. *Proceedings of the National Academy of Sciences of the United States of America*, *104*(8), 2750–2755. https://doi.org/10.1073/pnas.0610983104

Grishok, A., Pasquinelli, A. E., Conte, D., Li, N., Parrish, S., Ha, I., Baillie, D. L., Fire, A., Ruvkun, G., & Mello, C. C. (2001). Genes and mechanisms related to RNA interference regulate expression of the small temporal RNAs that control C. elegans developmental timing. *Cell*, *106*(1), 23–34. https://doi.org/10.1016/s0092-8674(01)00431-7

Grissa, I., Vergnaud, G., & Pourcel, C. (2007). The CRISPRdb database and tools to display CRISPRs and to generate dictionaries of spacers and repeats. *BMC Bioinformatics*, *8*(1), 172. https://doi.org/10.1186/1471-2105-8-172

Guo, H., Ingolia, N. T., Weissman, J. S., & Bartel, D. P. (2010). Mammalian microRNAs predominantly act to decrease target mRNA levels. *Nature*, *466*(7308), 835–840. https://doi.org/10.1038/nature09267

Guo, X., & Li, X.-J. (2015). Targeted genome editing in primate embryos. *Cell Research*, *25*(7), 767–768. https://doi.org/10.1038/cr.2015.64

He, D., Miao, H., Xu, Y., Xiong, L., Wang, Y., Xiang, H., Zhang, H., & Zhang, Z. (2014). MiR-371-5p Facilitates Pancreatic Cancer Cell Proliferation and Decreases Patient Survival. *PLoS ONE*, *9*(11), e112930. https://doi.org/10.1371/journal.pone.0112930

Hille, F., Richter, H., Wong, S. P., Bratovič, M., Ressel, S., & Charpentier, E. (2018). The Biology of CRISPR-Cas: Backward and Forward. *Cell*, *172*(6), 1239–1259. https://doi.org/10.1016/j.cell.2017.11.032

Horvath, P., & Barrangou, R. (2010). CRISPR/Cas, the Immune System of Bacteria and Archaea. *Science*, *327*(5962), 167–170. https://doi.org/10.1126/science.1179555

Huskova, H., Korecka, K., Karban, J., Vargova, J., Vargova, K., Dusilkova, N., Trneny, M., & Stopka, T. (2015). Oncogenic microRNA-155 and its target PU.1: An integrative gene expression study in six of the most prevalent lymphomas. *International Journal of Hematology*, *102*(4), 441–450. https://doi.org/10.1007/s12185-015-1847-4

Hutvágner, G., McLachlan, J., Pasquinelli, A. E., Bálint, E., Tuschl, T., & Zamore, P. D. (2001). A cellular function for the RNA-interference enzyme Dicer in the maturation of the let-7 small temporal RNA. *Science (New York, N.Y.)*, *293*(5531), 834–838. https://doi.org/10.1126/science.1062961

Chang, H., Yi, B., Ma, R., Zhang, X., Zhao, H., & Xi, Y. (2016). CRISPR/cas9, a novel genomic tool to knock down microRNA in vitro and in vivo. *Scientific Reports*, *6*(1), 22312. https://doi.org/10.1038/srep22312

Chiorazzi, N., Rai, K. R., & Ferrarini, M. (2005). Chronic lymphocytic leukemia. *The New England Journal of Medicine*, *352*(8), 804–815. https://doi.org/10.1056/NEJMra041720

Chronic lymphocytic leukaemia – atypical pleomorphic variant (mixed cell type)—CELL - Atlas of Haematological Cytology. (b.r.). Získáno 30. listopad 2020, z http://www.leukemia-cell.org/atlas/index.php?pg=images--mature-b-cell-neoplasms--chronic-lymphocytic-leukaemia--atypical-pleomorphic-variant-mixed-cell-type#1

Jurkovicova, D., Magyerkova, M., Kulcsar, L., Krivjanska, M., Krivjansky, V., Gibadulinova, A., Oveckova, I., & Chovanec, M. (2014). MiR-155 as a diagnostic and prognostic marker in hematological and solid malignancies. *Neoplasma*, *61*, 241–251. https://doi.org/10.4149/neo_2014_032

Kabadi, A. M., Ousterout, D. G., Hilton, I. B., & Gersbach, C. A. (2014). Multiplex CRISPR/Cas9-based genome engineering from a single lentiviral vector. *Nucleic Acids Research*, *42*(19), e147–e147. https://doi.org/10.1093/nar/gku749

Kistler, K. E., Vosshall, L. B., & Matthews, B. J. (2015). Genome Engineering with CRISPR-Cas9 in the Mosquito Aedes aegypti. *Cell Reports*, *11*(1), 51–60. https://doi.org/10.1016/j.celrep.2015.03.009

Kluiver, J., Poppema, S., de Jong, D., Blokzijl, T., Harms, G., Jacobs, S., Kroesen, B.-J., & van den Berg, A. (2005). BIC and miR-155 are highly expressed in Hodgkin, primary mediastinal and diffuse large B cell lymphomas. *The Journal of Pathology*, *207*(2), 243–249. https://doi.org/10.1002/path.1825

Lander, E. S. (2016). The Heroes of CRISPR. *Cell*, *164*(1–2), 18–28. https://doi.org/10.1016/j.cell.2015.12.041

Lu, D., Nakagawa, R., Lazzaro, S., Staudacher, P., Abreu-Goodger, C., Henley, T., Boiani, S., Leyland, R., Galloway, A., Andrews, S., Butcher, G., Nutt, S. L., Turner, M., & Vigorito, E. (2014). The miR-155-PU.1 axis acts on Pax5 to enable efficient terminal B cell differentiation. *The Journal of Experimental Medicine*, *211*(11), 2183–2198. https://doi.org/10.1084/jem.20140338

Makarova, K. S., & Koonin, E. V. (2015). Annotation and Classification of CRISPR-Cas Systems. *Methods in molecular biology (Clifton, N.J.)*, *1311*, 47–75. https://doi.org/10.1007/978-1-4939-2687-9_4

Marraffini, L. A., & Sontheimer, E. J. (2010). CRISPR interference: RNA-directed adaptive immunity in bacteria and archaea. *Nature Reviews Genetics*, *11*(3), 181–190. https://doi.org/10.1038/nrg2749

Mashima, R. (2015). Physiological roles of miR-155. *Immunology*, *145*(3), 323–333. https://doi.org/10.1111/imm.12468

Mohanraju, P., Makarova, K. S., Zetsche, B., Zhang, F., Koonin, E. V., & van der Oost, J. (2016). Diverse evolutionary roots and mechanistic variations of the CRISPR-Cas systems. *Science*, *353*(6299), aad5147. https://doi.org/10.1126/science.aad5147

Mojica, F. J. M., & Montoliu, L. (2016). On the Origin of CRISPR-Cas Technology: From Prokaryotes to Mammals. *Trends in Microbiology*, *24*(10), 811–820. https://doi.org/10.1016/j.tim.2016.06.005

Morange, M. (2015). What history tells us XXXVII. CRISPR-Cas: The discovery of an immune system in prokaryotes. *Journal of Biosciences*, *40*(2), 221–223. https://doi.org/10.1007/s12038-015-9532-6

O'Connell, R. M., Zhao, J. L., & Rao, D. S. (2011). MicroRNA function in myeloid biology. *Blood*, *118*(11), 2960–2969. PubMed. https://doi.org/10.1182/blood-2011-03-291971

O'Donnell, K. A., Wentzel, E. A., Zeller, K. I., Dang, C. V., & Mendell, J. T. (2005). C-Myc-regulated microRNAs modulate E2F1 expression. *Nature*, *435*(7043), 839–843. https://doi.org/10.1038/nature03677

Pagotto, S., Veronese, A., Soranno, A., Lanuti, P., Marco, M. D., Russo, M. V., Ramassone, A., Marchisio, M., Simeone, P., Franchi, P. E. G., Palka, G., Costantini, R. M., Croce, C. M., & Visone, R. (2018). *Hsa-miR-155-5p* drives aneuploidy at early stages of cellular transformation. *Oncotarget*, *9*(16), 13036–13047. https://doi.org/10.18632/oncotarget.24437

Pospisil, V., Vargova, K., Kokavec, J., Rybarova, J., Savvulidi, F., Jonasova, A., Necas, E., Zavadil, J., Laslo, P., & Stopka, T. (2011). Epigenetic silencing of the oncogenic miR-17-92 cluster during PU.1-directed macrophage differentiation: Pu.1/Egr2/Jarid1b pathway silences miR-17-92 cluster. *The EMBO Journal*, *30*(21), 4450–4464. https://doi.org/10.1038/emboj.2011.317

Rodriguez, A., Vigorito, E., Clare, S., Warren, M. V., Couttet, P., Soond, D. R., van Dongen, S., Grocock, R. J., Das, P. P., Miska, E. A., Vetrie, D., Okkenhaug, K., Enright, A. J., Dougan, G., Turner, M., & Bradley, A. (2007). Requirement of bic/microRNA-155 for

Normal Immune Function. *Science*, *316*(5824), 608–611. https://doi.org/10.1126/science.1139253

Seiffert, M., Stilgenbauer, S., Döhner, H., & Lichter, P. (2007). Efficient nucleofection of primary human B cells and B-CLL cells induces apoptosis, which depends on the microenvironment and on the structure of transfected nucleic acids. *Leukemia*, *21*(9), 1977–1983. https://doi.org/10.1038/sj.leu.2404863

SHAO, M., XU, T.-R., & CHEN, C.-S. (2016). The big bang of genome editing technology: Development and application of the CRISPR/Cas9 system in disease animal models. *Zoological Research*, *37*(4), 191–204. https://doi.org/10.13918/j.issn.2095-8137.2016.4.191

Thai, T.-H., Calado, D. P., Casola, S., Ansel, K. M., Xiao, C., Xue, Y., Murphy, A., Frendewey, D., Valenzuela, D., Kutok, J. L., Schmidt-Supprian, M., Rajewsky, N., Yancopoulos, G., Rao, A., & Rajewsky, K. (2007). Regulation of the germinal center response by microRNA-155. *Science (New York, N.Y.)*, *316*(5824), 604–608. https://doi.org/10.1126/science.1141229

Vargova, K., Pesta, M., Obrtlikova, P., Dusilkova, N., Minarik, L., Vargova, J., Berkova, A., Zemanova, Z., Michalova, K., Spacek, M., Trneny, M., & Stopka, T. (2017). MiR-155/miR-150 network regulates progression through the disease phases of chronic lymphocytic leukemia. *Blood Cancer Journal*, *7*(7), e585–e585. https://doi.org/10.1038/bcj.2017.63

Vigorito, E., Kohlhaas, S., Lu, D., & Leyland, R. (2013). miR-155: An ancient regulator of the immune system. *Immunological Reviews*, *253*(1), 146–157. https://doi.org/10.1111/imr.12057

Vigorito, E., Perks, K. L., Abreu-Goodger, C., Bunting, S., Xiang, Z., Kohlhaas, S., Das, P. P., Miska, E. A., Rodriguez, A., Bradley, A., Smith, K. G. C., Rada, C., Enright, A. J., Toellner, K.-M., MacLennan, I. C. M., & Turner, M. (2007). MicroRNA-155 Regulates the Generation of Immunoglobulin Class-Switched Plasma Cells. *Immunity*, *27*(6), 847–859. https://doi.org/10.1016/j.immuni.2007.10.009

Wallace, J. A., Kagele, D. A., Eiring, A. M., Kim, C. N., Hu, R., Runtsch, M. C., Alexander, M., Huffaker, T. B., Lee, S.-H., Patel, A. B., Mosbruger, T. L., Voth, W. P., Rao, D. S., Miles, R. R., Round, J. L., Deininger, M. W., & O'Connell, R. M. (2017). MiR-155 promotes FLT3-ITD–induced myeloproliferative disease through inhibition of the

interferon response. *Blood*, *129*(23), 3074–3086. https://doi.org/10.1182/blood-2016-09-740209

Wang, B., Li, D., Rodriguez-Juarez, R., Farfus, A., Storozynsky, Q., Malach, M., Carpenter, E., Filkowski, J., Lykkesfeldt, A. E., & Kovalchuk, O. (2018). A suppressive role of guanine nucleotide-binding protein subunit beta-4 inhibited by DNA methylation in the growth of anti-estrogen resistant breast cancer cells. *BMC Cancer*, *18*(1), 817. https://doi.org/10.1186/s12885-018-4711-0

Wang, H., Yang, H., Shivalila, C. S., Dawlaty, M. M., Cheng, A. W., Zhang, F., & Jaenisch, R. (2013). One-Step Generation of Mice Carrying Mutations in Multiple Genes by CRISPR/Cas-Mediated Genome Engineering. *Cell*, *153*(4), 910–918. https://doi.org/10.1016/j.cell.2013.04.025

Wang, Y., Mao, H., Hao, Q., Wang, Y., Yang, Y., Shen, L., Huang, S., & Liu, P. (2012). Association of expression of XIAP-associated factor 1 (XAF1) with clinicopathologic factors, overall survival, microvessel density and cisplatin-resistance in ovarian cancer. *Regulatory Peptides*, *178*(1–3), 36–42. https://doi.org/10.1016/j.regpep.2012.06.005

Winter, J., Jung, S., Keller, S., Gregory, R. I., & Diederichs, S. (2009). Many roads to maturity: MicroRNA biogenesis pathways and their regulation. *Nature Cell Biology*, *11*(3), 228–234. https://doi.org/10.1038/ncb0309-228

Xiao, M., Li, J., Li, W., Wang, Y., Wu, F., Xi, Y., Zhang, L., Ding, C., Luo, H., Li, Y., Peng, L., Zhao, L., Peng, S., Xiao, Y., Dong, S., Cao, J., & Yu, W. (2016). MicroRNAs activate gene transcription epigenetically as an enhancer trigger. *RNA Biology*, *14*(10), 1326–1334. https://doi.org/10.1080/15476286.2015.1112487

Xu, L., Leng, H., Shi, X., Ji, J., Fu, J., & Leng, H. (2017). MiR-155 promotes cell proliferation and inhibits apoptosis by PTEN signaling pathway in the psoriasis. *Biomedicine & Pharmacotherapy*, *90*, 524–530. https://doi.org/10.1016/j.biopha.2017.03.105

Yoshino, H., Yonemori, M., Miyamoto, K., Tatarano, S., Kofuji, S., Nohata, N., Nakagawa, M., & Enokida, H. (2017). MicroRNA-210-3p depletion by CRISPR/Cas9 promoted tumorigenesis through revival of TWIST1 in renal cell carcinoma. *Oncotarget*, *8*(13), 20881–20894. https://doi.org/10.18632/oncotarget.14930

Yu, H., Xu, W., Gong, F., Chi, B., Chen, J., & Zhou, L. (2017). MicroRNA-155 regulates the proliferation, cell cycle, apoptosis and migration of colon cancer cells and targets

CBL. *Experimental and Therapeutic Medicine*, *14*(5), 4053–4060. https://doi.org/10.3892/etm.2017.5085

Internet resources

https://www.genecards.org/

http://www.mirbase.org/

https://rnacentral.org/